



Research Article

Performance analysis of microchannel heat sink with flow disrupting pins

V. P. GAIKWAD^{*1}, S. S. MOHITE²

¹Research Scholar, Government College of Engineering, Karad, India, 415124, Faculty, Textile and Engineering Institute, Ichalkaranji, India, Affiliated to Shivaji University, Kolhapur, India

²College of Engineering Pune, 411005, India

ARTICLE INFO

Article history

Received: 22 August 2020

Accepted: 02 March 2021

Keywords:

Pin-enhanced Microchannel; Enhancement Factor; Pressure Drop; Thermo-hydraulic Performance; Electronics Cooling

ABSTRACT

Study of thermo-hydraulic characteristics of a novel microchannel heat sink having flow disrupting pins is numerically and experimentally carried out in this paper. Cylindrical pins are inserted from top cover into the rectangular microchannel instead of the conventional technique of pin-fins originating from the base of microchannel. Initially, the effect of pin diameter on the thermo-hydraulic performance is studied and the optimum pin diameter is established, later on thermo-hydraulic performance of pin enhanced microchannel heat sink (PE-MCHS) is compared with conventional microchannel heat sink (MCHS). Of the five pin diameters studied, pin having 0.2mm diameter (relative pin diameter $\gamma = 0.4$) gives the best performance. Both conventional MCHS and PE-MCHS are subjected to heat flux ranging from $65\text{W}/\text{cm}^2$ to $200\text{W}/\text{cm}^2$ and cooled by water flowing at Reynolds number ranging from 745 to 1500. The presence of pins disturbs the velocity distribution completely and increases the heat transfer capacity of the MCHS accompanied by higher pressure drop penalty. The average enhancement factor obtained by this technique is 1.24. Correlations showing the effect of channel width to pin diameter ratio (Wc/Dp) on Nusselt number (Nu) and friction factor (f) are proposed.

Cite this article as: Gaikwad V. P, Mohite S. S. Performance analysis of microchannel heat sink with flow disrupting pins. J Ther Eng 2022;8(3):402–425.

INTRODUCTION

Electronics has influenced the day to day activities of all human beings. Electronic components are becoming more and more compact in size for example the computers have moved from desktop to wrist watch. Electronic packaging is an art of providing a suitable environment to

the electronic products for continuous and reliable performance. Ergonomics, manufacturing, maintenance, thermal management, shock and vibration are some of the mechanical design aspects to be considered in electronics packaging. Since millions of circuits are placed in a small

*Corresponding author.

*E-mail address: gvinayak2002@gmail.com

This paper was recommended for publication in revised form by Regional Editor Erman Aslan



space, large amount of heat (100 – 200 W/cm²) is generated. Cooling system performance is one of the major concerns in integrated circuit design. A number of cooling methods have been explored by several researchers. Air cooled systems have already reached their maximum heat removing capacity. As mentioned by Gaikwad et al. [1] “Liquid cooled microchannel heat sink (MCHS) is one of the most appropriate cooling systems for such applications.” They have high heat load removing capacity from a small space. High surface to volume ratio, low coolant inventory, ability to be mounted on chip to form monolithic configuration are other characteristics of MCHS. Tuckerman and Pease [2] were the first researchers to study MCHS, after them a number of researchers have made attempts to optimize the microchannel dimensions and advance the performance of conventional parallel (MCHS). Knight et al. [3] formulated the governing equations in dimensionless form for thermo-hydraulic performance of heat sink for laminar and turbulent flow. They then formulated a method to find dimensions of microchannel heat sink having minimum thermal resistance for laminar and turbulent flow. The newly developed method was used to find the dimensions of MCHS for their respective boundary conditions reported by Tuckerman and Pease, Goldberg and Philips and found that the thermal resistance decreased by 10 to 35 percent.

Due to the short length scales of microchannel, the liquid flow type remains laminar. As the liquid passes quickly through the channel, only the liquid near the wall surface gets heated while the one in the core region is unaffected by the heat. More heat transfer takes place at the entrance region due to thermo-hydraulic entrance length, while the rate of heat transfer reduces along the channel length resulting in a) increase in surface temperature along the length of microchannel, b) thickening of boundary layer and c) sensible heat gain by the coolant. Thus, the liquid core part has less capacity to absorb heat generated at the channel base region and from the channel walls. Near the outlet region, high temperature gradient is present between wall surface and liquid in channel core which indicates less heat absorbed by the liquid. This is due to the thick boundary layer and is a major roadblock for the attainment of higher thermal efficiencies in microchannel. Steinke and Kandlikar [4] studied the applicability of already established enhancement methods of conventional channels for microchannels and minichannels. Flow disruptions, channel curvature, secondary flows, out of plane mixing are some of the methods reviewed. Of the various performance enhancement methods suggested, flow disruptions are widely studied. Some of the enhancement methods employed in MCHS by researchers are listed in Table 1.

Kosar and Peles [5] were the first to experimentally study the thermo-hydraulic performance of an array of pin-fins extending over the entire height of microchannels. Various designs having inline or staggered arrangement, pin-fin density were studied. Densely populated pin fins with

staggered arrangement accomplished higher heat transfer coefficient compared to inline configuration and larger pin fins spacing. Colgan et al. [6] created staggered and continuous strip fins on silicon and integrated them with chip to form single chip module. The module subjected to heat flux of 300 Watt per sq.cm demonstrated the pressure drop less than 35 kPa and thermal resistance of 10.5 °C-sq. mm/Watt. The fins in staggered form at a pitch of 75 or 100 μm showed superior performance than continuous fin designs having equivalent geometries. Hong and Cheng [7] obtained the optimal offset strip fin for constraints of low wall temperature, high heat flux and low pumping power. They designed the modules having different fin pitch to fin length ratios, and fin numbers and studied its effect on the performance. They concluded that of all the cases studied, the case having fin interval to fin length ratio of one is the optimal design. Shafeie et al. [8] numerically analysed the pin-fin heat sinks and pin-finned MCHS having oblique or staggered pattern and different heights and compared the performance with simple MCHS. For medium and high pumping powers, the finned MCHS performance was lower than simple MCHS, but for low pumping power conditions, the new MCHS showed slightly better performance over conventional MCHS.

Xie et al. [9] studied the effect of distance between side wall and pin-fin column near side wall in a pin-finned microchannel arrangement on heat transfer and heat transfer. They studied three designs having Gap to Diameter ratio of 0.6, 1.0 and 1.4 subjected to heat flux of 10 W/cm² and Reynolds number in the range of 13 to 202. They found that the gap distance severely influences the velocity field, flow and temperature distributions in the microchannel. For a fixed Reynolds number, and for increase in gap distance, the pressure drop decreases continuously while the heat transfer initially increases and then reduces. They concluded that the case having ratio of one shows superior thermal performance. They also developed correlations showing effect of sidewall to pin distance on friction factor and Nusselt number.

Heat generated by 2016s IC was removed by heat sink with micro-pins designed by Rubio-Jimenez et al. [10]. They proposed a fin density that varies along the length for uniform temperature distribution in IC chip. Pin shapes viz. circle, square, elliptical and flat were analyzed for laminar flow condition. They concluded that flat shaped fins had the best performance of all pin shapes. The design was able to dissipate heat of 2016s IC at pumping power of 0.04 W with a pressure drop of 20 kPa. The temperature gradient obtained by this design is one fourth of that obtained by conventional MCHS.

Use of pin fins inside the microchannel as the method of enhancement was studied by Yadav et al. [11] Three different configurations of pin-fins placement viz. upstream, downstream and uniformly spaced pin-fins throughout the length of channel were studied. They deduced that the

overall enhancement factor is greater than one for all three configurations. Optimisation of the enhanced microchannels was carried out by using univariate search technique. Various parameters of pin-fin are optimized. Heat transfer enhancement of 160% is obtained for optimised design. Jia et al. [12] created a fan shaped fin inserted in the microchannel for performance enhancement. They also created different configurations based on fin positions and then optimised the various parameters of pin-fin and microchannel. They found the optimum parameters as relative fin diameter of 0.375, relative fins space of 1, and relative fin height of 0.04 which for Reynolds number of 637 attained an enhancement factor of 1.55.

Ansari and Kim [13] proposed a combination of microchannel and pin-fins (Table 1) for heat removal from single hotspot generated by microprocessor with heterogeneous power distributions. Conjugate heat transfer analysis results showed that when subjected to background heat flux of 50 Watt per sq.cm and hotspot heat flux of 200 Watt per sq.cm and flow rate corresponding to Reynolds number of 200, the design attained 30.6% lower temperature rise with increased pumping power of 11.7%. For a fixed Reynolds number the hybrid design can withstand 50% higher heat flux at the hotspot compared to conventional design.

Chai et al. [14] experimentally and numerically investigated the performance enhancement in microchannels which have periodic expansion and constriction. They considered various parameters such as conjugate heat transfer, entrance effect, multi-channel effect, and viscous heating in the investigation. Experimental results show that Nusselt number and apparent friction factor predicted numerically are in good agreement. The thermal performance improved owing to the new design by a factor of 1.8 compared to conventional MCHS. For lower flow rates ($Re < 300$), the pressure drop is lower than conventional MCHS but increases rapidly and is higher for $Re > 300$. Pankaj Kumar [15] numerically studied trapezoidal shaped microchannels with rectangular and semi-circular grooved structure. They observed that trapezoidal shaped microchannel showed 12% enhancement in performance than rectangular microchannel. The presence of grooved structure on the walls of channel further enhances the performance by 28%. The enhancement is due to separation and redevelopment of thermal and hydraulic boundary layers.

Vijay et al. [16] altered the design of parallel microchannels to converging and diverging type and performed numerical and experimental study of the convective heat transfer in such microchannels. Microchannel with 8° angle of divergence and 156 μm hydraulic diameter were etched on silicon wafer for both converging and diverging modes. The microchannel was applied a heat flux of less than 10 W/cm^2 with water as coolant at Reynolds number of 30 to 274. They concluded that compared to diverging microchannel, in converging microchannel there is 35% higher heat transfer. Also the pumping power required for converging and

diverging microchannel is significantly less compared to parallel microchannel.

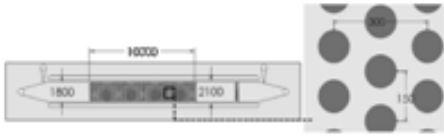
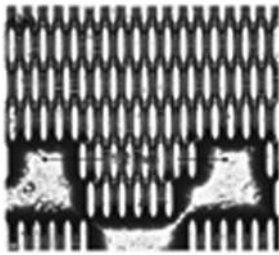
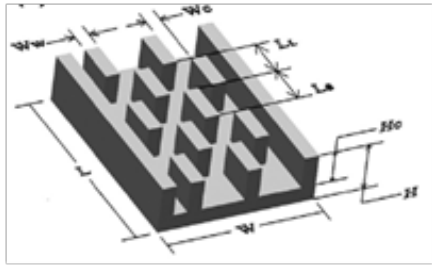
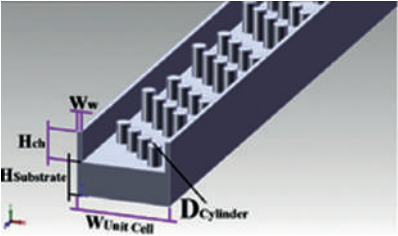
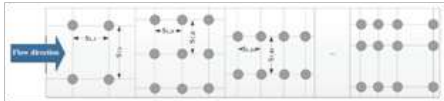
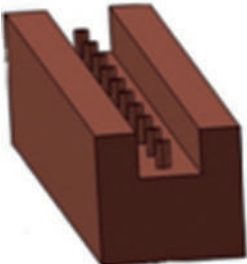
Yong and Teo [17] numerically studied microchannels having converging and diverging passages subjected to uniform wall temperature of 350 K and for Reynolds number ranging from 50 to 200. Two designs of converging diverging passages one with constant curvature and other with sinusoidal form for the same cross section were studied. The unique design creates a couple of symmetric vortices which help in improving the thermo-hydraulic performance by 60 percent.

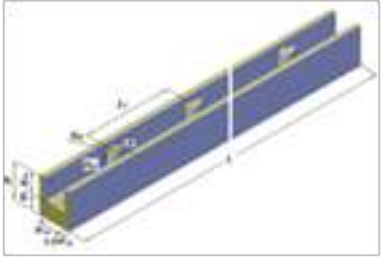
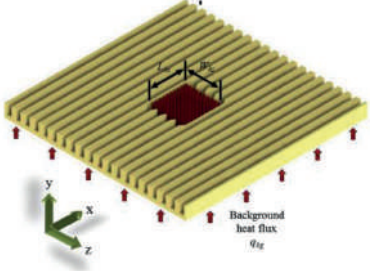
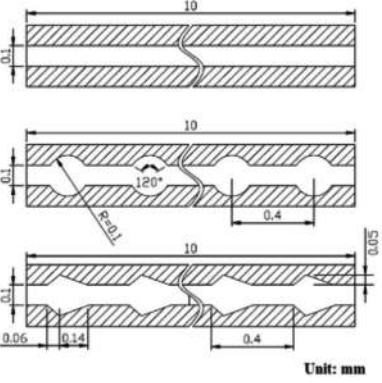
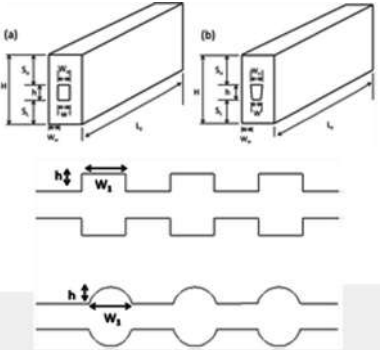
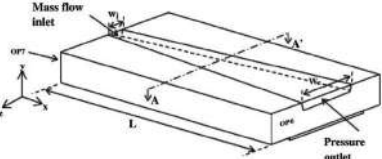
Lan et al. [18] incorporated dimples and protrusions on the side walls of microchannel and studied the change in flow and thermal performance. Twelve cases were created by varying the span-wise (P) and stream-wise (S) pitch. The smallest periodic domain (SPD) is subjected to heat flux of 50 W/cm^2 and cooled by water for various Reynolds number. For the thermal performance (η) for these cases, they noted that: (1) The microchannel with dimple and protrusion show better performance than the one with dimple only microchannel; (2) The microchannel with smaller stream-wise pitch have better performance; (3) The microchannel with staggered dimple placement have better performance than the microchannel with non-staggered dimples.

Xu et al. [19] numerically investigated microchannel with dimples on the bottom surface subjected to heat flux of 100 W/cm^2 and flow at Reynolds number of 500. The results yield drop in surface temperature by 3.2K, rise in Nusselt number by 15% and rise in pressure drop by 2%. Lu and Zhai [20] combined vortex generators and dimples in a microchannel heat sink to improve its thermal performance. Three pairs of vortex generators are evenly placed along the length while the dimples are placed in the downstream of vortex generators. They concluded that the combination of vortex generator and dimples can enhance the thermal performance by 23 to 60 % with increase in penalty of friction factor of 22 to 54 %. The design having vortex generator of height ratio of 0.6 and attack angle of 45° gives the best thermal performance.

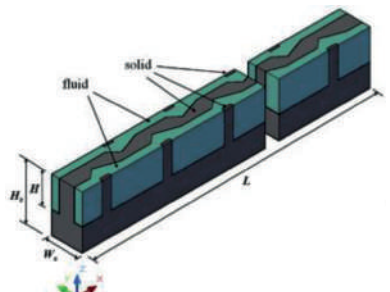
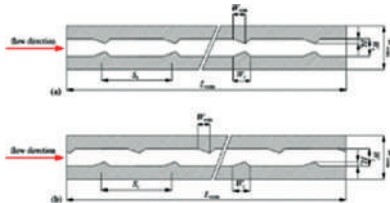
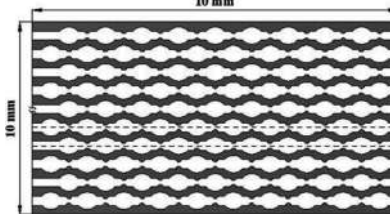
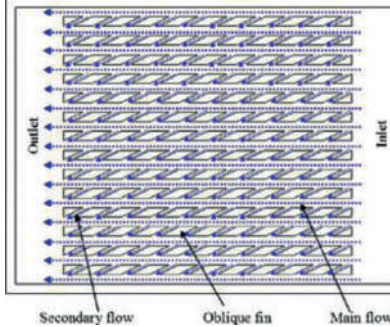
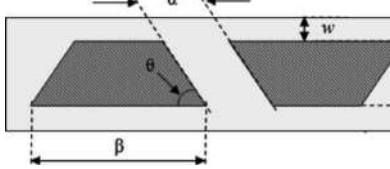
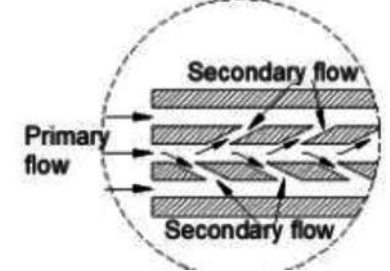
Xie et al. [21] designed five different cases of microchannels with structural based multistage bifurcations and numerically investigated their flow and thermal performance. Only half of the single microchannel is modeled using planar symmetry, its bottom surface is subjected to heat flux of 24.5 W/cm^2 and its performance is studied for various inlet Reynolds numbers ranging from 230 to 560. They observed that secondary flows are not generated for any case even for highest inlet velocity. The bifurcations result in very high pressure drop, the pressure drop ratio ($\Delta P/\Delta P_0$) for case 3 with conventional microchannel (case 0) reaching a value of 10. For the same case highest Nusselt number is reported. The overall thermal resistance is lowest for case 3 with the enhancement factor of 1.78. They concluded that single stage bifurcations having longer length (case 1) can give better performance if designed properly.

Table 1: Enhancement methods studied by earlier researchers

Sr. No.	Author	Figure	MC dimensions (microns)	Heat flux range/Const. Temp. (W/cm ²)/(K)	Reynolds number/ Flow rate	Concluding remarks
1	Kosar and Peles[5]		99.5 pin diameter	3.8 to 167	14 to 112	Nu = 7
2	Colgan et al.[6]		W = 75; H = 195	300	26 to 282	$\frac{h}{k_0} = 1.3$
3	Hong and Cheng[7]		W = 57; H = 300	100, 200	75	Optimum fin length to fin interval K = 1
4	Shafeie et al.[8]		D = 80, 100; H = 1000	Ts = 358 K	1 to 9 ml/min	Rise in Heat flux removed = 250%
5	Xie et al.[9]		D _p = 500; H _p = 500; G = 300 to 700	10	Re = 13 to 202	$\eta = 1.14$
6	Rubio-Jimenez et al. [10]		W = 50; H = 100	100	1 to 5 ml/s	$\frac{\Delta T_0}{\Delta T} = 4.2$
7	Yadav et al.[11]		W = 231; H = 713	100, 200	Re = 400 to 1200	$\eta = 1.73$

Sr. No.	Author	Figure	MC dimensions (microns)	Heat flux range/Const. Temp. (W/cm ²)/(K)	Reynolds number/Flow rate	Concluding remarks
8	Jia et al.[12]		W = 200; H = 200	100	Re = 150 to 640	$\eta = 1.5$
9	Ansari & Kim[13]		$W_{ch} = 250$; $H_{ch} = 500$; $D_{pin} = 120$	50 & 300 (Hotpot)	Re = 200 to 1000	R_{th} reduced by 30.6%
10	Chai et al.[14]		W = 100; H = 200	60	Re = 150 to 800	$\frac{Nu}{Nu_0} = 1.8$
11	Pankaj-kumar[15]		W = 231; H = 713	100	Re = 150-720	$\frac{h}{k_0} = 1.28$
12	Vijay Duryodhan [16]		W1 = 252; W2 = 3052	0.3 to 9.5	Re = 80 to 180	$\frac{h}{k_0} = 1.35$

Sr. No.	Author	Figure	MC dimensions (microns)	Heat flux range/Const. Temp. (W/cm ²)/(K)	Reynolds number/ Flow rate	Concluding remarks
14	Yong and Teo[17]		$D_h = 200$	$T_s = 350$ K	50 to 200	$\eta = 1.6$
15	Lan et al.[18]		$W = 50;$ $H = 200$	50	Re = 100 to 900	$\eta = 1.12$ to 4.77
16	Xu et al.[19]		$W = 500;$ $H = 500$	100	Re = 500	$\eta = 1.16$
17	Lu and Zhai[20]		$W = 200;$ $H = 400;$ $dm = 160$	100	Re = 167 to 834	$\eta = 1.17$ to 1.28
18	Xie et al. [21]		$W = 315;$ $H = 400;$	24.5	Re = 230 to 560	$\frac{R_{th}}{N_{th0}} = 1.78$
19	Shen et al.[22]		$W = 298;$ $H = 400$	100	Re = 100 to 1000	$\eta = 1.14$
20	Chai et al. [32]		$W = 100;$ $H = 200;$	100	Re = 187 to 715	$\frac{Nu}{Nu_0} = 2.03$

Sr. No.	Author	Figure	MC dimensions (microns)	Heat flux range/Const. Temp. (W/cm ²)/(K)	Reynolds number/Flow rate	Concluding remarks
21	Li et al.[25]		W = 200; H = 200	100	Re = 160 to 640	$\eta = 1.55$
22	Chai et al. [26]		W = 100; H = 200	100	Re = 443	$\frac{Nu}{Nu_0} = 2.15$
23	Xia et al.[33]		W = 200	100	Re = 250 to 610	$\eta = 5.44$
24	Lee et al.[27]		W ₁ = 500; W ₂ = 300; H = 1500	100	Re = 325 to 780	$\eta = 1.6$
25	Kuppusamy [28]		W = 300; H = 300	100	m = 0.001 kg/s	$\eta = 1.46$
26	Gaikwad et al. [29]		W = 500; H = 1500;	100	Re = 652 to 1309	$\eta = 1.4$ to 1.85

Shen et al. [22] used a single vertical rib in the microchannel but varied its distance from outlet end and studied the effect of the position of the vertical rib. They concluded that the introduction of rib the thermal resistance decreases by 27% and the thermal performance increased by 14% for rib nearest to the outlet.

Zunaid et al. [23] introduced semi cylindrical projections in the microchannel and compared the thermo-hydraulic characteristics with conventional microchannel. They found that the semi cylindrical projections help in improvement in thermal performance but with added pressure drop penalty. Belhadj et al. [24] employed two different types of cavities in the channel wall of cylindrical and triangular shape to create periodic increase and decrease in cross section and studied its effect on thermo-hydraulic performance. They concluded that the Nusselt number maximum increased by 36 percent whereas the pressure drop increased by 44 percent.

Li et al. [25] developed sidewall flow obstructions and rectangular ribs in the microchannel. The ribs are placed in the middle of flow region while the cavities are created on the sidewalls as shown in Table 1. “The thermo-hydraulic performance of this new design is studied numerically subjected to a heat flux of 100 Watt per sq. cm and cooled by water at Reynolds number 160 to 640” [1]. They conclude that the design has more enhanced performance than the other enhancement designs. The maximum enhancement factor achieved is 1.619 at Re of 500.

Chai et al. [26] employed triangular ribs mounted on sidewalls and studied its hydro-thermal characteristics. The ribs were aligned or offset with respect to each other and two different rib-widths were used to create four MCHS designs. The MCHS were subjected to heat flux of 100W/cm² and flow rate corresponding to Reynolds number of 443. They concluded that the aligned triangular ribs created a converging diverging channel type while the offset ribs created a wavy channel type. Both have similar thermal performance but the offset ribs design has much smaller pressure drop. The offset rib design having rib-width of 0.1mm obtained a 2.15 times higher Nusselt number than conventional parallel MCHS.

Lee et al. [27] deployed inclined secondary channels(250 μm) which connect the primary channels (500 μm). The inclined channel deflects a small share of the fluid into adjacent channel. The replacement of a continuous fin into fin with connecting channels results in break and re-initialization of the thermal boundary layer, increases mixing of fluid which helps to boost heat transfer. The experimental investigation on MCHS is performed for heat flux of 100 Watt per sq. cm and cooled by water with flow rates corresponding to Reynolds numbers of 325–780. “They reported that the average Nusselt number of such fins increased by 103% from 11.3 to 22.9” [1]

Kuppusamy et al. [28] placed triangular shaped mixers in the walls of microchannels and optimised the

design by considering two different designs and two different flow directions. They obtained design that gives higher heat transfer performance with no increased pressure drop. They conclude that the micro-mixer design increases the thermal performance along with reduced pressure drop.

Gaikwad et al. [29] connected the neighbouring parallel channels by secondary channels forming a leaf venation type network. Numerical analysis to assess the thermo-hydraulic performance of this new design was done and results compared with conventional microchannel. They concluded that there was a minimum 40 percent rise in thermo-hydraulic performance. Use of microchannel as cross flow heat exchanger was done by Meral et al. [30]. Use of ribs as passive enhancement technique was done by Madani et al. [31]

Many researchers have explored the means of enhancing the performance of MCHS. Utilization of pin-fins in microchannel has been studied by some researchers. In case of macro-channels, it is already proved that the introduction of pin-fins inside the channel improves its thermal performance. But manufacturing feasibility is a major challenge for use of pin-fins in microchannel field. Placing of pin fins of size smaller than width of microchannel though not impossible, but, difficult to fabricate. A cost effective method of improving the microchannel performance enhancement is needed. In this paper, we introduce the pins from the top cover instead of pin-fins rising from the base which can be done at a very small additional cost. The inserted pins help in disrupting the flow and enhance the performance of MCHS. The numerical study of the pin enhanced MCHS is carried out subjected to various heat flux and cooled by water flowing at different flow rates. Initially, numerical analysis of pin-enhanced microchannel heat sink (PE-MCHS) of various pin diameters is performed and optimum pin diameter is obtained. The effect of pins on thermal and fluid flow is discussed next. The performance of optimum PE-MCHS is compared with that of conventional (parallel) microchannel heat sink (MCHS). Experimental and numerical results are compared and found satisfactory. Later, correlations are derived for Nusselt number and friction factor for channel width to pin diameter ratio.

NUMERICAL STUDY

The footprint area for both conventional MCHS and PE-MCHS is 25mm × 25mm. The number of channels is 24. To reduce the computational time, only a single channel is considered for simulation (Figure 1) for both MCHS. Figure 2 shows the schematic of a single channel containing the pins. The cylindrical pins (total quantity four) are uniformly spaced along the entire length of the microchannel. The dimensions of the conventional MCHS and pin enhanced microchannel heat sink (PE-MCHS) are given in Table 2. Based on the earlier research work by Yadav et al.[11] and Jia et al. [12], in which the pin-fins placed along

the entire channel length show better performance, the number and the location of pins are decided. Four pins are placed uniformly along the length of microchannel (pitch 5.00 mm). The top of microchannel is covered by a acrylic plate to restrict the fluid movement and heat loss through the top. The pins are inserted from the acrylic cover plate instead of the conventional method of pins rising from the base of the microchannel. Constant heat flux is applied at the bottom of MCHS. The material of pins and microchannel is copper.

Simulation Model

The computational domain for both MCHS (Figure 3(a) and 3(b)) consists of a single channel with half width

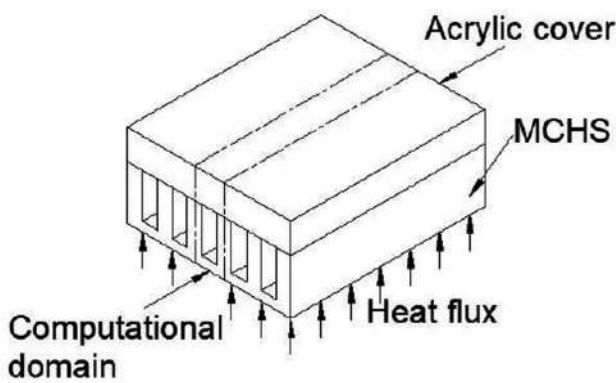


Figure 1: Computational domain derived from MCHS.

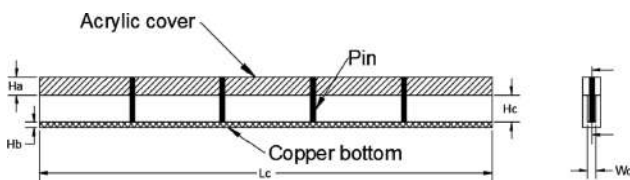


Figure 2: Cross section of PE-MCHS.

of neighbouring walls. The PE-MCHS domain is made up of one fluid region and two solid regions, the first is microchannel and the second is top cover and pins inserted from top cover. The space in between these solids is occupied by the fluid region. “Three dimensional numerical analysis was done using the commercial CFD software ANSYS FLUENT. The numerical analysis is done by solving the conservation of mass, momentum and energy equations (Eq. 1 to 4). The three dimensional, double precision, solver is used with SIMPLE scheme for pressure-velocity coupling. For the spatial discretization scheme, second order is used for the pressure equation while second order upwind scheme is used for both momentum and energy equations. In solution controls, the under-relaxation factors used are: 0.5 for pressure and for momentum, and 1.0 for density, momentum and energy. In the monitors, the residual convergence criterion of 10-6 is set for all equations. Copper with constant thermal conductivity of 387.6 W/mK is chosen as the solid material for pins and microchannel. Water with temperature dependent properties is assigned to fluid”[1]. Following assumptions are made for the numerical analysis:

Table 2: Dimensions of MCHS

Characteristics	Conventional MCHS	Pin Enhanced MCHS (PE-MCHS)
Material	Copper	Copper
Footprint L × W (mm)	25 × 25	25 × 25
Channel width W_c (μm)	500	500
Wall width W_w (μm)	500	500
Height of Channel H_c (μm)	1500	1500
Aspect ratio (H_c/W_c)	3.0	3.0
Acrylic cover height H_a (μm)	1000	1000
Copper base Height H_b (μm)	300	300
Pin fin diameter D_p (μm)	--	100 - 300

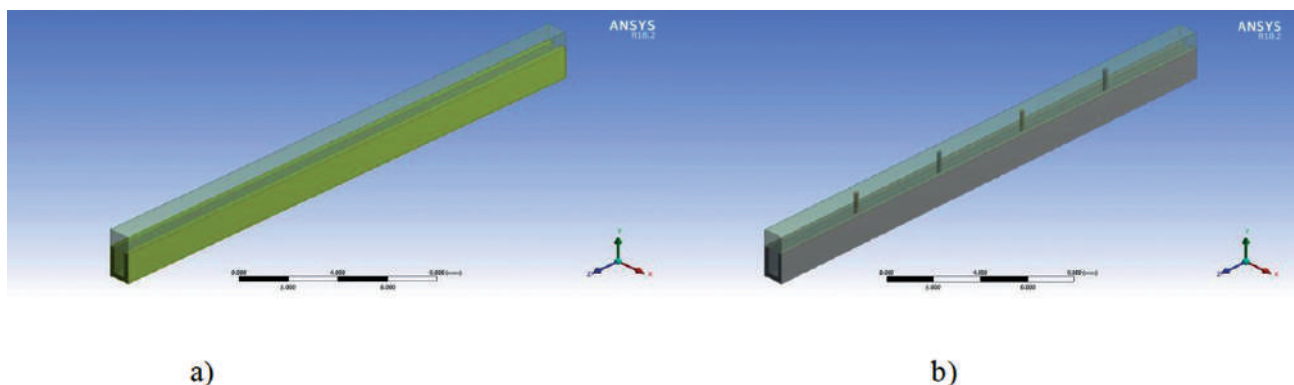


Figure 3: Simulation model for a) conventional MCHS b) PE-MCHS.

- Fluid is incompressible.
- Flow is laminar, steady and Newtonian.
- Radiation heat transfer is neglected.
- No-slip boundary condition at wall.

The governing equations are as follows:

Continuity equation:

$$\nabla \cdot (\rho \vec{v}) = 0 \quad (1)$$

Momentum equation:

$$\nabla \cdot (\rho \vec{v} \vec{v}) = -\nabla P + \nabla \cdot (\mu \nabla \vec{v}) \quad (2)$$

Energy equation for liquid:

$$\nabla \cdot (\rho \vec{v} (C_p T)) = \nabla \cdot (k \nabla T) \quad (3)$$

Energy equation for solid:

$$\nabla \cdot (k \nabla T) = 0 \quad (4)$$

Boundary Conditions

The simulation model for both conventional MCHS and PE-MCHS are applied with different boundary conditions. “At inlet, a constant velocity (range 0.63 m/s to 1.26 m/s) is applied to inlet region equivalent to the flow rate for single channel (Reynolds number range 745 to 1500). The temperature of fluid at the inlet is 308 K. Heat flux (65 Watt/cm² to 200 Watt/cm²) is applied to the bottom of the MCHS. Pressure outlet condition is applied at the outlet. Adiabatic conditions are applied to all the remaining outer surfaces”[1].

Grid Independence

The conventional MCHS is meshed using hex elements while the PE-MCHS domain is meshed by hex and wedge elements. The wedge elements are used due to the cylindrical shape of pin (Figure 4). To eliminate the errors due to coarse mesh, the grid independence test was performed (Table 3). The number of elements for conventional and PE-MCHS are increased and corresponding bottom surface

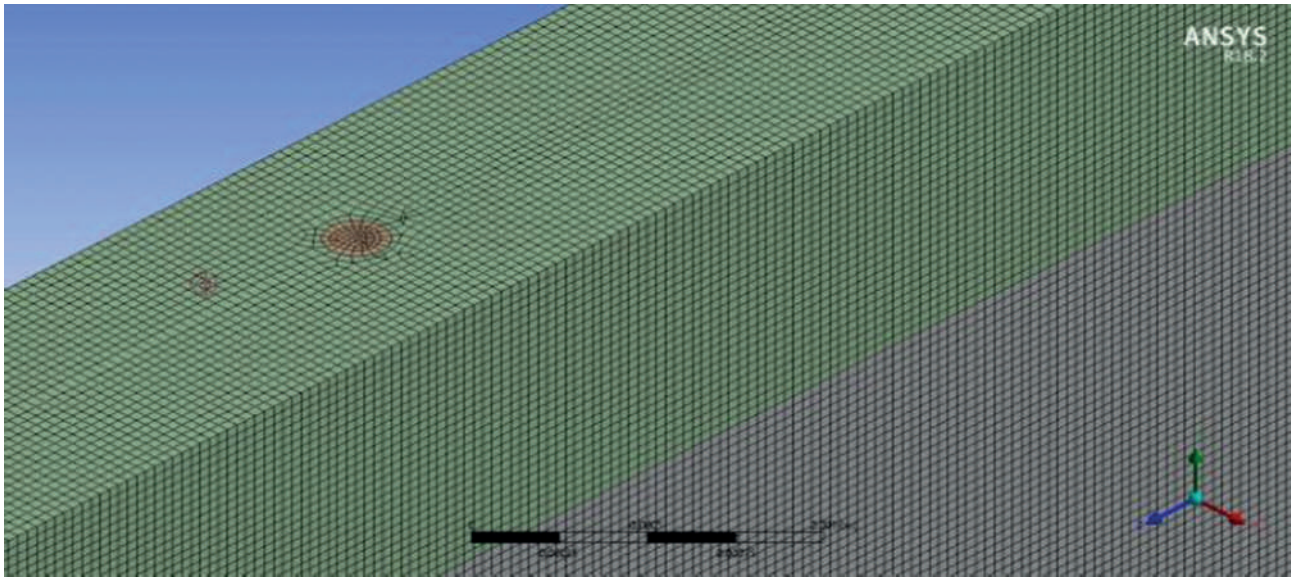


Figure 4: Mesh around the pin using wedge and hexahedral elements in PE-MCHS.

Table 3: Grid independence test summary

Grid System	No. of elements		PE-MCHS	Max. Bottom Surface Temp. Variation %
	Conventional MCHS	Max. Bottom Surface Temp. Variation %		
I	179550		216134	
II	1437084	0.18	1494852	0.92
III	3737652	0.43	3792163	0.05

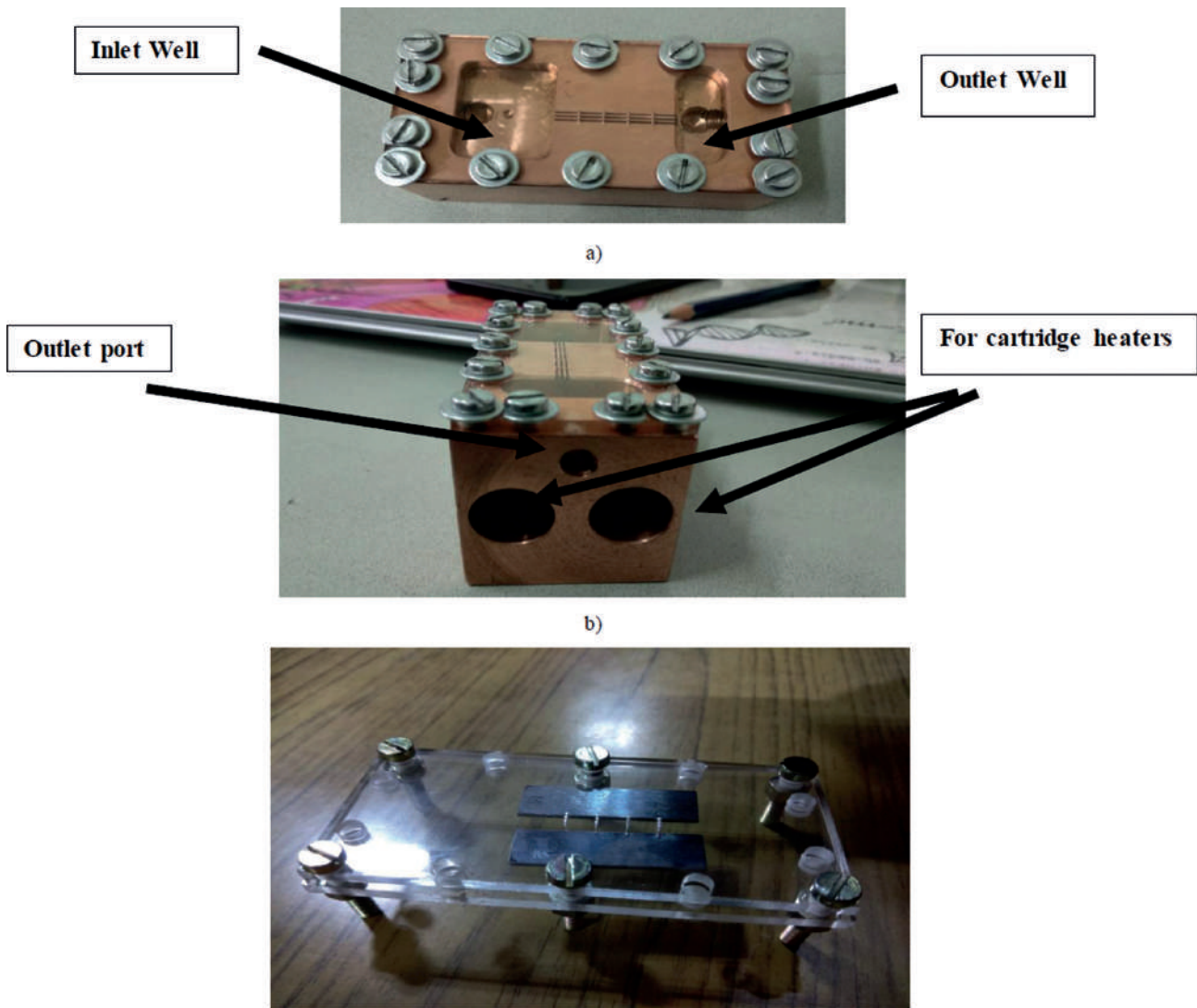


Figure 5: a) Microchannel heat sink with three channels connected with inlet and outlet well b) location of cartridge heaters c) Use of slip gauge for inserting the pins in acrylic cover.

temperature and other parameters were noted. Since the maximum variation in bottom surface temperature is less than 0.5 percent for changing from the grid system II to III, grid system II was selected for further analysis.

EXPERIMENTAL STUDY

As mentioned earlier, the footprint of the microchannel design is 25mm × 25mm and contains 25 microchannels each of width 0.5mm and the thickness of wall is 0.5mm. For experimental study a set of three microchannels with pins inserted from top cover was manufactured as shown in Figure 5 a) and b). The test piece is a copper block which houses the cartridge type heaters, inlet and outlet port, inlet and outlet well, and cavities for thermocouple. The acrylic

cover is fitted on the top of microchannel with screws as shown in Figure 5 a). Cavity for inserting the cartridge heaters is shown in Figure 5 b). Holes are drilled from the sides for thermocouple which measure the temperature below the microchannels. The test piece is insulated by glass-wool cover to reduce the heat loss to surrounding. Slip gauges were used to insert the pins through the acrylic cover as shown in Figure 5 c).

The experimental setup is as shown in Figure 6. A peristaltic pump (Masterflex make) is used to supply metered quantity of de-ionised water to the microchannel test piece which is heated by two cartridge heaters with the help of DC power supply. Temperature is noted at various locations in the test piece with thermocouples (Omega make) and at the inlet and outlet of water circuit.

Table 4: Uncertainty of various parameters measured

Parameters	Fractional uncertainty
Pressure 1 mm of Hg	0.011
Power q_w W	0.0002
T_s °C	0.002
T_i °C	0.004
T_o °C	0.003
h_{ave} (W/cm ² K)	0.0092
Nu	0.030
η	0.082

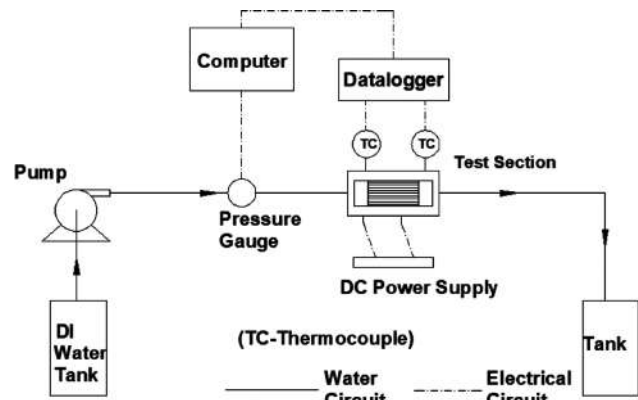


Figure 6: Schematic layout of experimental setup.

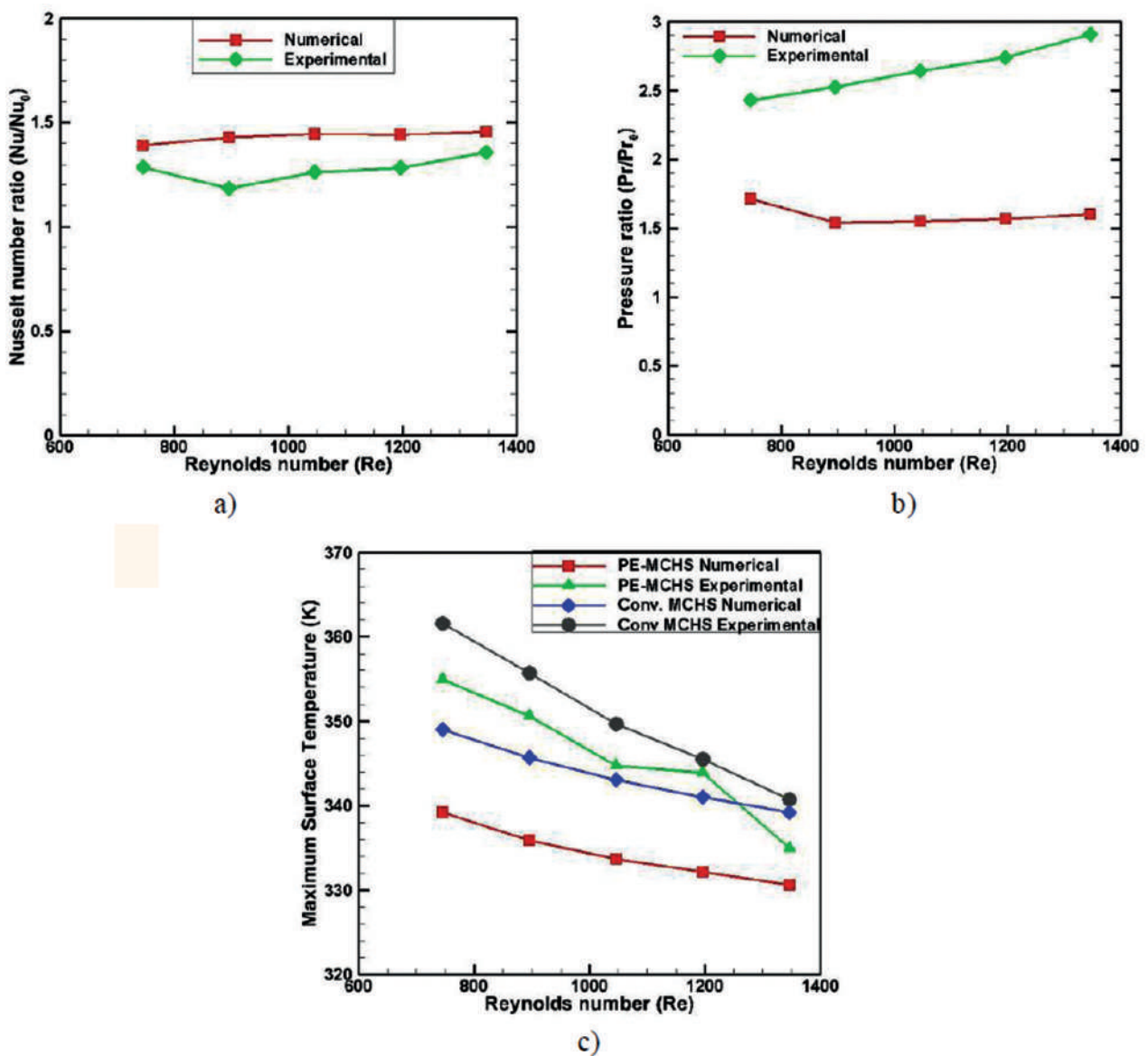


Figure 7: Comparison of numerical and experimental performance of Conventional and Enhanced MCHS a) Effect of Reynolds number on Nusselt number ratio b) Effect of Reynolds number on pressure ratio c) Effect of Reynolds number on Surface temperature.

Thermocouples are connected to data acquisition system (Dewesoft make) which is further recording the data in the computer. Pressure gauge (Keller make) is used to measure the pressure of the heat sink.

The test piece can be treated as conventional and enhanced MCHS by changing the acrylic cover. The test piece was subjected to heat flux of 65–200 Watts per sq. cm and cooled by de-ionised water at various flow rates and the temperature and pressure readings are noted. The experimental uncertainties are as shown in Table 4.

For the same test conditions, the experimental performance of conventional and enhanced MCHS is compared with numerical performance by comparing the Nusselt number ratio and pressure ratio. Figure 7 shows the comparison of numerical and experimental analysis for both MCHS subjected to heat flux of 100 watts per sq. cm and cooled by water at various flow rates. Nusselt number ratio (Figure 7a) are in good agreement with each other. Pressure ratio comparison (Figure 7b) has more deviation which can be attributed to location of pressure gauge which measures pressure losses in entire fluid passage system instead of pressure drop measured across microchannel in numerical analysis. Effect of flow rate on maximum surface temperature is shown in Figure 7c). Maximum surface temperature decreases with increase in flow rate for all cases. The temperature is lower in enhanced MCHS compared to its corresponding conventional MCHS. Overall the experimental and numerical results are in good agreement with each other.

DATA REDUCTION

For uniformity of calculation, the Reynolds number based on inlet velocity is considered and is given by the expression:

$$Re = \frac{\rho U_{in} D_h}{\mu} \quad (5)$$

where ρ , U_{in} , μ are fluid density, inlet velocity, and dynamic viscosity of water respectively. D_h is the hydraulic diameter of the channel and is given by:

$$D_h = \frac{4 * Area}{Perimeter} = \frac{4H_c W_c}{(2H_c + W_c)} \quad (6)$$

Only three sides of channel contribute to the heat transfer since the top cover is of acrylic. Hence perimeter includes only three sides of channel.

“The thermal performance can be studied by finding the heat transfer coefficient and Nusselt number. The expression for average heat transfer coefficient is given by:

$$h_{ave} = \frac{q_w A_{bottom}}{A_{con} (T_s - T_f)} \quad (7)$$

where q_w is the heat flux applied to the bottom of MCHS, A_{bottom} is the bottom surface area where heat flux is applied, A_{con} is the contact surface area between solid and fluid, T_s , T_f are the average surface temperature and fluid mean temperature respectively extracted by volume average temperature for solid and fluid domain respectively” [1].

The Nusselt number is obtained by

$$Nu = \frac{h_{ave} D_h}{k_f} \quad (8)$$

where h_{ave} is average heat transfer coefficient, D_h is hydraulic diameter and k_f is the thermal conductivity of fluid.

Friction factor is a function of fluid velocity at minimum cross-section (U) and is given by [34]

$$f = \frac{2\Delta p}{N_x \rho U^2} \quad (9)$$

where N_x is the number of pins in a row, ρ is the density of fluid and Δp is the drop in pressure in the entire channel.

The thermal performance of MCHS increases with introduction of pins but the pressure drop due to the pins also increases. The Nusselt number ratio is the comparison of Nusselt number of enhanced MCHS (Nu) and conventional MCHS (Nu_0). The pressure drop ratio is the ratio of pressure drop of enhanced MCHS (Δp) and conventional MCHS (Δp_0). The enhancement factor thus is a function of Nusselt number ratio and pressure drop ratio (ref. [11]) and is given by

$$\eta = \frac{Nu/Nu_0}{\left(\frac{\Delta p}{\Delta p_0}\right)^{0.333}} \quad (10)$$

RESULTS AND DISCUSSION

VALIDATION:

The numerical simulation is validated with the experimental work done by Qu and Mudawar [35] and the numerical results of microchannel having similar dimensions by Lee et al. For comparing the results with Qu and Mudawar [35], the microchannel designed is subjected to heat flux of 100 W/cm² and cooled by water flowing at Reynolds number 140 to 550. Figure 8 a) shows the variation of pressure drop with Reynolds number while Figure 8 b) shows the difference in outlet and inlet temperature with respect to Reynolds number. Figure 8 a) and b) show good agreement between numerical and experimental results.

The performance of conventional MCHS in current simulation is compared with earlier work having same dimensions and boundary conditions. The conventional MCHS of Lee et al. [27] has the width of 500 μ m and depth of 1500 μ m. The bottom surface temperature measured

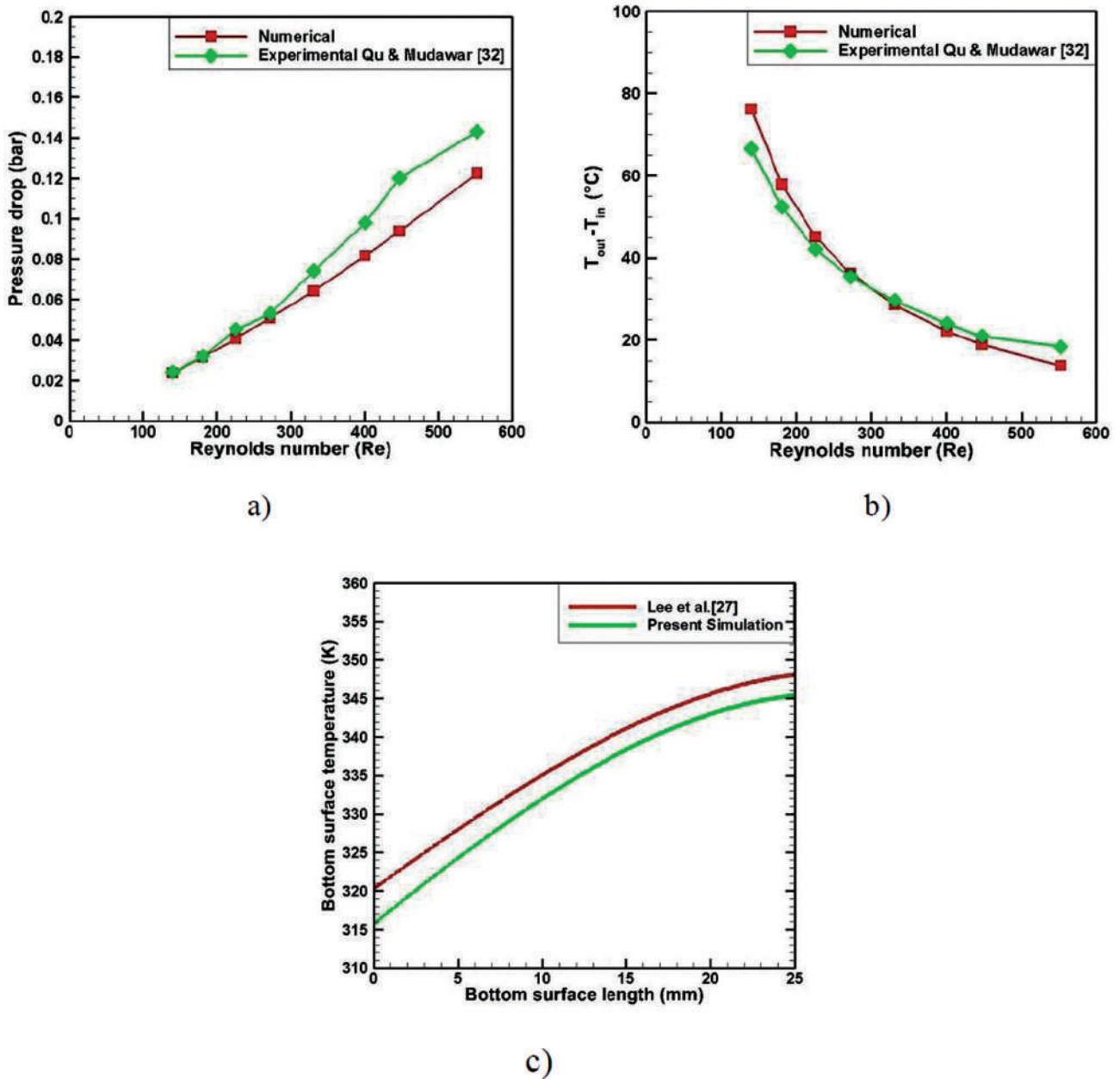


Figure 8: Validation of numerical results with a) experimental results of Qu and Mudawar of Pressure drop b) Temperature difference at inlet and outlet c) Bottom surface temperature comparison with microchannel with oblique fins of Lee et al.

along a straight line along the channel length of Lee et al. [27] is compared for same heat flux (65 W/cm^2) and flow rate (inlet velocity 0.3 m/s) with the conventional MCHS of current simulation (Figure 8). The maximum variation in the aforementioned temperature is 1.4 percent which signifies the accuracy and reliability of the current simulation.

To justify the new design, its performance is compared with that of MCHS with pin-fins which rise from the base. In microchannel with pins rising from base (PF-MCHS), the pin-fins help in a) conducting the heat into the water

stream in the channel and b) flow disruption. In microchannel with pins inserted from top cover (PE-MCHS), the pins help in only flow disruption and are not conducting the heat from base surface to water stream. Numerical simulation for the two designs is performed for pin of 0.2 mm diameter and is subjected to various heat flux and flow rates. Figure 9 shows the variation of pressure drop and maximum bottom surface temperature for different flow rates for both pin designs subjected to heat flux of 100 W/cm^2 . There is rise in pressure drop with higher flow rates for

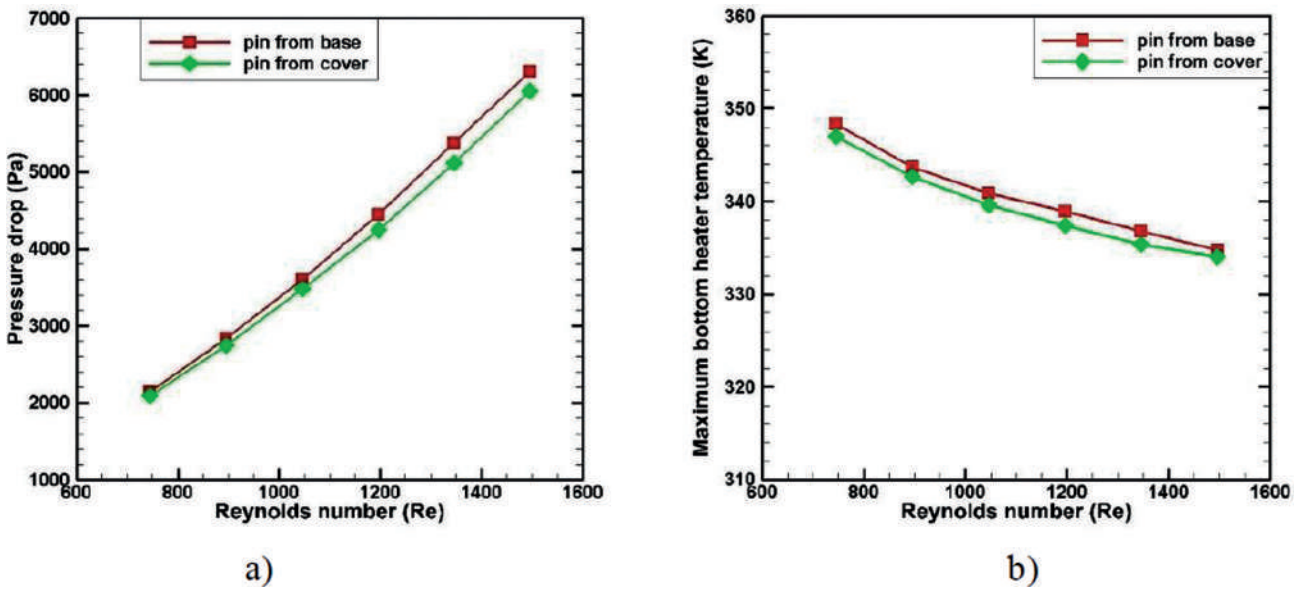


Figure 9: Comparison of a) Pressure drop and b) maximum bottom surface temperature for pins inserted from top and pins originating base.

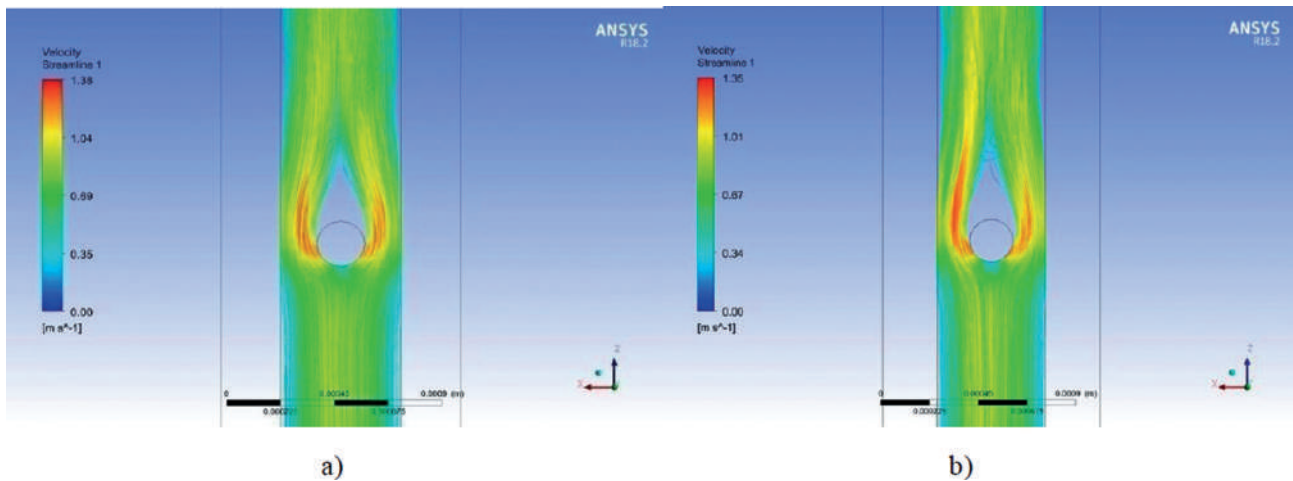


Figure 10: Streamlines around a single pin for a) Pin inserted from top and b) Pins originating from the base on ZX plane (Y = 1mm) at Reynolds number of 745.

both pin enhanced MCHS, the difference in pressure drop for both designs is less than 5 percent. The maximum bottom surface temperature decreases at higher in flow rates for both pin designs, the difference between two designs is less than 0.5 percent. Figure 10 shows the streamlines around a single pin for both pin designson ZX plane (Y=1mm) at Reynolds number of 745; there is not much difference in the flow pattern, maximum velocity, and wake formation for both pin designs. Figure 11 shows the temperature contour for a single pin and the channel base for both designs subjected to heat flux of 100 W/cm² and Reynolds number

of 745. The continuity in temperature is visible for pins rising from the base while for pins inserted from top there is marked jump in temperature between base and pin. But the temperature variation within the pin is similar for both designs. Thus the performance of pins inserted from the top cover is similar as that of pin fins rising from the base.

Optimum Pin Diameter

Effect of pin diameter on thermal and hydraulic performance is discussed here. Pins having diameter of 0.125,

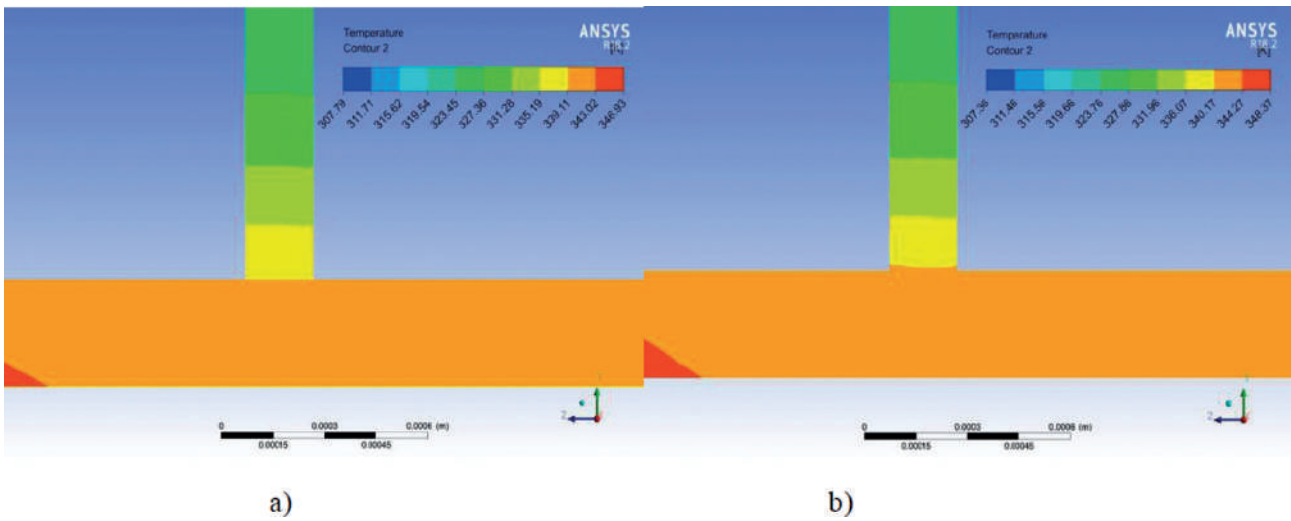


Figure 11: Temperature contour around a single pin and channel base for a) Pin inserted from top and b) Pin originating from the base.

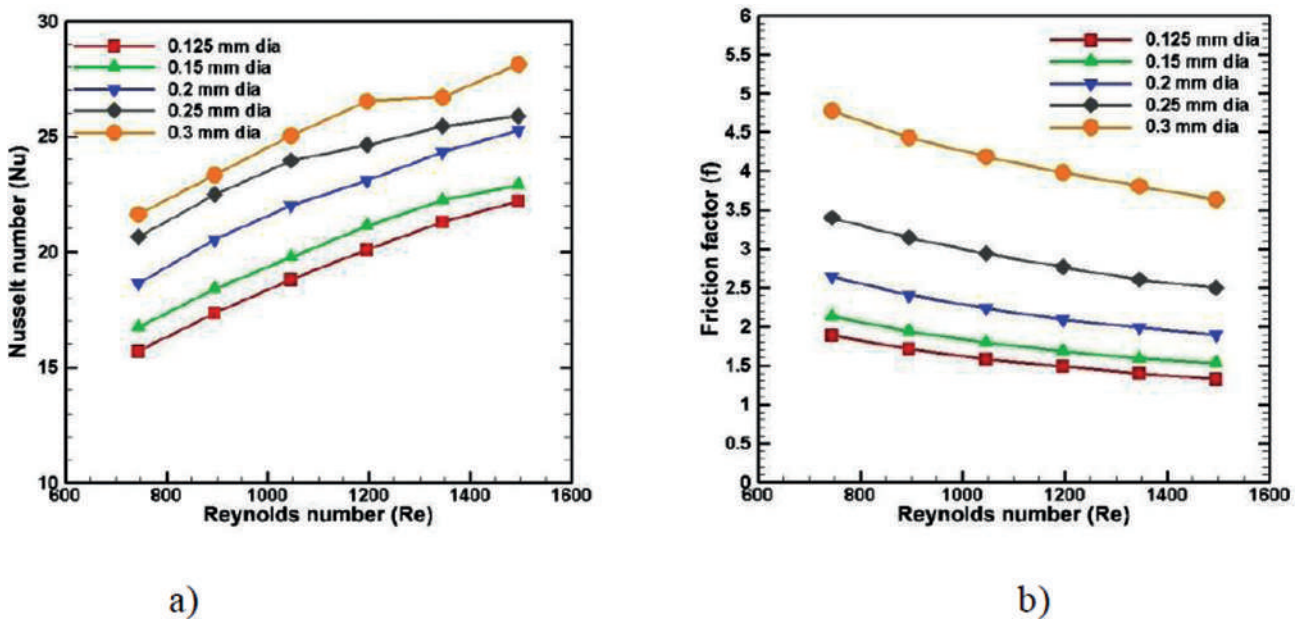


Figure 12: Comparison of a) Nusselt number and b) friction factor for various pin diameters.

0.15, 0.2, 0.25 and 0.3mm (relative pin diameter $\gamma = D_p/W_c$) are considered for comparison. Figure 12a) shows the variation of Nusselt number and 9b) shows friction factor for various Reynolds number for different pin diameters. For all pin diameters, the Nusselt number increments at higher flow rates, while the friction factor reduces at higher flow rates. Highest values of Nusselt number and friction factor are reported by pins of 0.3 mm diameter ($\gamma = 0.6$). The enhancement factor which is a function of Nusselt number and pressure drop (eq. 10) helps to judge the thermo-hydraulic performance of flow disrupting pins.

Figure 13 shows the variation of enhancement factor for different values of Reynolds number of pins of various diameters. For a given Reynolds number, the enhancement factor increases with increase in pin diameter up to 0.2mm diameter ($\gamma = 0.4$) and decreases for 0.25 ($\gamma = 0.5$) and 0.3mm diameter ($\gamma = 0.6$). The enhancement factor for 0.25 ($\gamma = 0.5$) show nonlinear relation with increase in Reynolds number. Its average enhancement factor is less than that of 0.2mm diameter ($\gamma = 0.4$) for the entire flow range. The effect of pin diameter in a microchannel can be observed in Figure 14 which shows the streamlines around a single

pin. The increase in pin diameter results in reduction in space between pins and channel walls causing increase in flow velocity and increase in pressure drop. Maximum velocity observed is 1.79 m/s for 0.3mm pin diameter while the minimum velocity observed is 1.18 m/s for 0.125 mm pin diameter ($\gamma = 0.25$). The wake size also increases with increase in pin diameter resulting in higher pressure drop. Comparison of thermo-hydraulic performance reveals that the optimum pin diameter is 0.2 mm ($\gamma = 0.4$) as further increase or decrease in pin diameter, the thermo-hydraulic performance reduces.

Thermo-Hydraulic Performance of PEMCHS

Both conventional and pin enhanced MCHS (0.2mm pin diameter) are subjected to heat flux of 65, 100, 150 and

200 Watt per sq.cm, cooled by water having inlet Reynolds number ranging from 745 to 1500. Figure 15 compares the Nusselt number for different flow rates for heat flux of 100 W/cm² and 200 W/cm². Nusselt number increases rapidly for PE-MCHS than conventional MCHS with increase in Reynolds number. As expected, the performance of PE-MCHS is much better than conventional MCHS. This can be attributed to the additional contact surface of pin in PE-MCHS, break in boundary layer and mixing of cooling liquid which is absent in conventional MCHS. The insertion of pins improves the performance but with pressure drop penalty. As shown in Figure 16, there is rise in pressure drop with higher flow rates for both MCHS, but for PE-MCHS the pressure drop rises rapidly and is nearly two times that for the conventional MCHS at Reynolds number of 1500. For heat flux of 200 W/cm² the pressure drop is slightly less than for heat flux of 100 W/cm². The results indicate the accomplishment of pins in their function of flow disruption.

The flow disruption caused by the pins results in mixing of fluid. This is more evident in temperature contours in the fluid region at vertical planes 1mm downstream from the pins as shown in Figure 17 (a) through 17(e). The temperature of core region of fluid increases after each pin and after the fourth pin, very less fluid has the base temperature of 308 K. Figure 18 shows the temperature of fluid at the outlet in both MCHS. The conventional MCHS shows core fluid region at base temperature of 308 K and is unaffected by heat transfer at the walls and the temperature difference within the fluid region is 52 K. The PE-MCHS shows no fluid with base temperature of 308 K and the temperature difference within the fluid region is 38 K. The temperature variation at different locations in the microchannel shows that water from the core region is getting mixed with water near solid surfaces and thus more heat is being absorbed by water.

Figure 19 shows the temperature variation along the vertical plane at the center of channel for the heat flux of 100 W/cm² and Reynolds number of 745 for conventional

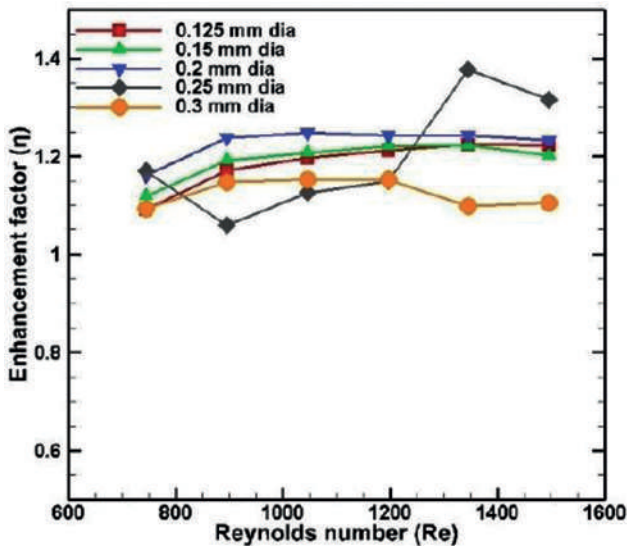


Figure 13: Enhancement factor comparison for various pin diameters.

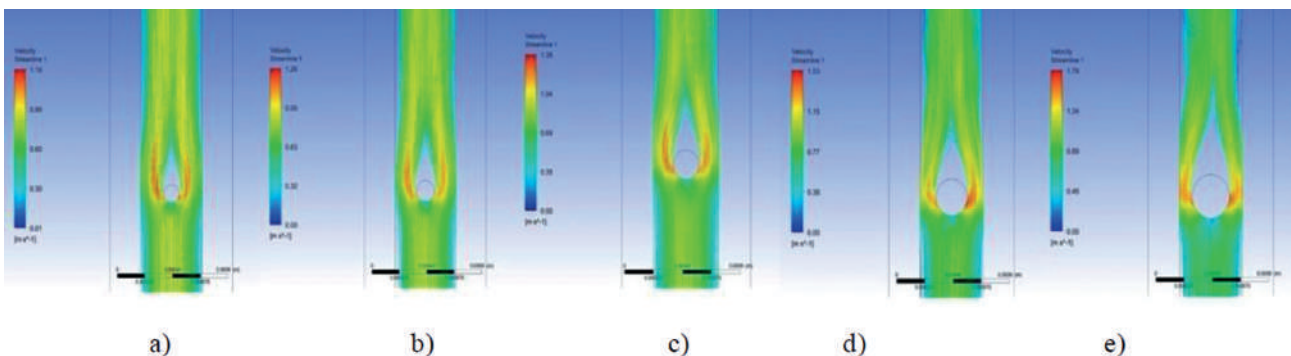
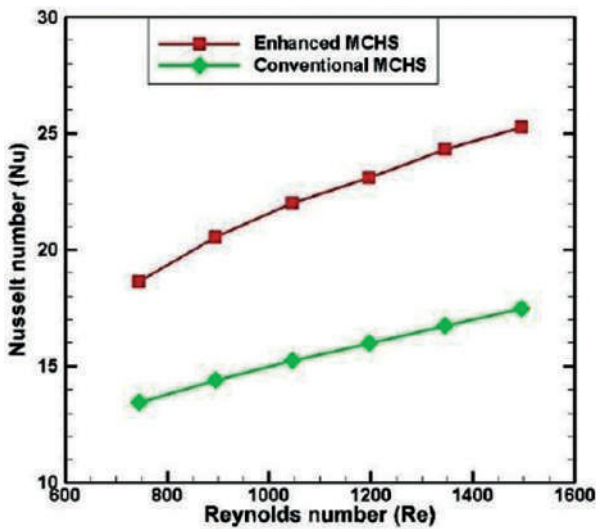
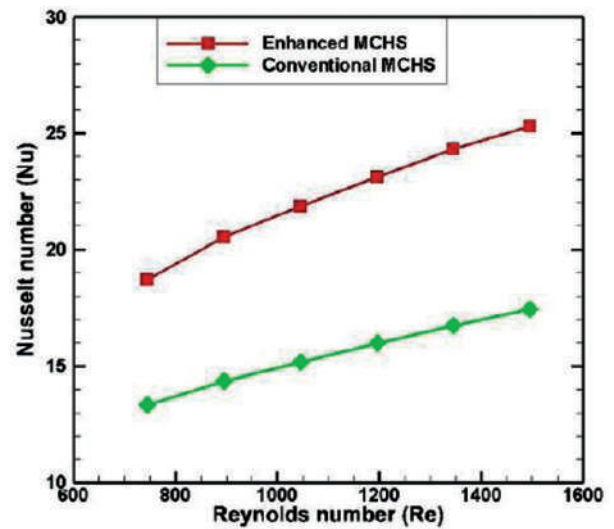


Figure 14: Streamlines around a single pin having pin diameter of a) 0.125mm b) 0.15mm c) 0.20mm d) 0.25mm and e) 0.3mm on ZX plane ($Y = 1\text{mm}$) at Reynolds number of 745.

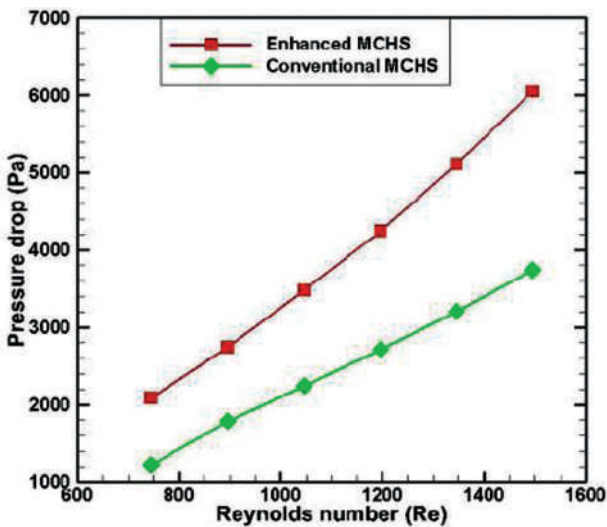


a)

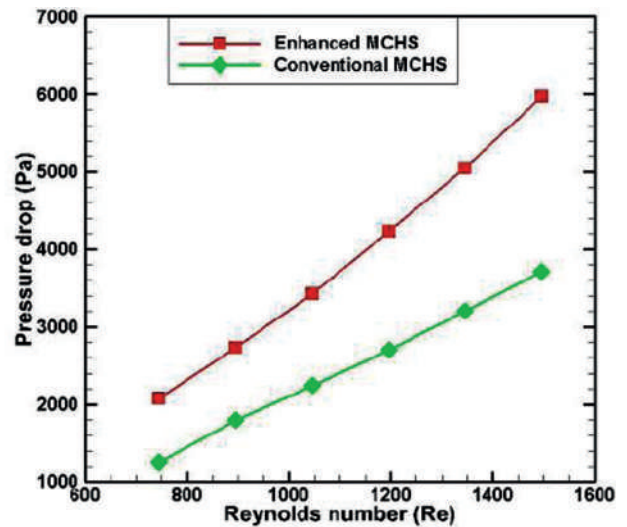


b)

Figure 15: Nusselt number variation with respect to Reynolds number for heat flux of a) 100W/cm² b) 200 W/cm².



a)



b)

Figure 16: Pressure drop variation with respect to Reynolds number for heat flux of a) 100W/cm² b) 200W/cm².

MCHS and PE-MCHS. The direction of coolant flow is shown by the arrows. In conventional MCHS the temperature of fluid remains constant along the entire length. In PE-MCHS, the temperature increases by 12 K. The rise in temperature in PE-MCHS is due to the flow disrupting pins which induce mixing of fluid at different temperatures.

Variation of velocity and temperature along the channel wall for both conventional and PE-MCHS is shown in

Figure 20 (a) and (b) respectively. Close observation shows that the velocity distribution is same for both MCHS in the entrance region. It drastically changes afterwards. For conventional MCHS, the velocity remains nearly constant indicating a developed flow, but in PE-MCHS, the velocity fluctuates between high near the pins to low after the pins. The presence of pins creates a narrow area through which the fluid flows at high velocity. The velocity variation

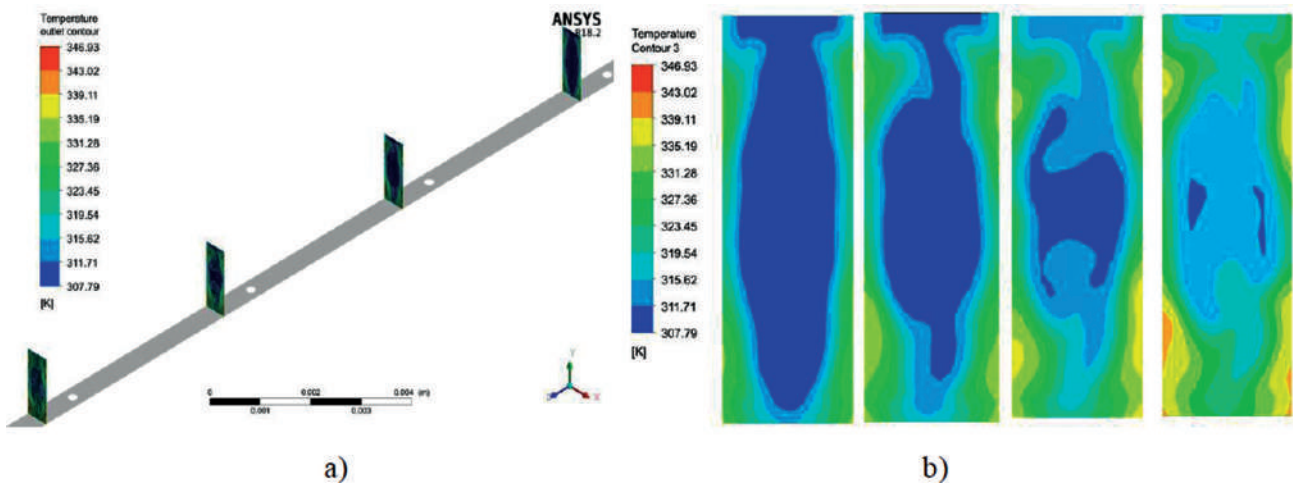


Figure 17: Temperature contour plot in the a) entire fluid region (channel cross-section) at 1mm distance downstream from each pin for heat flux of $100\text{W}/\text{cm}^2$.

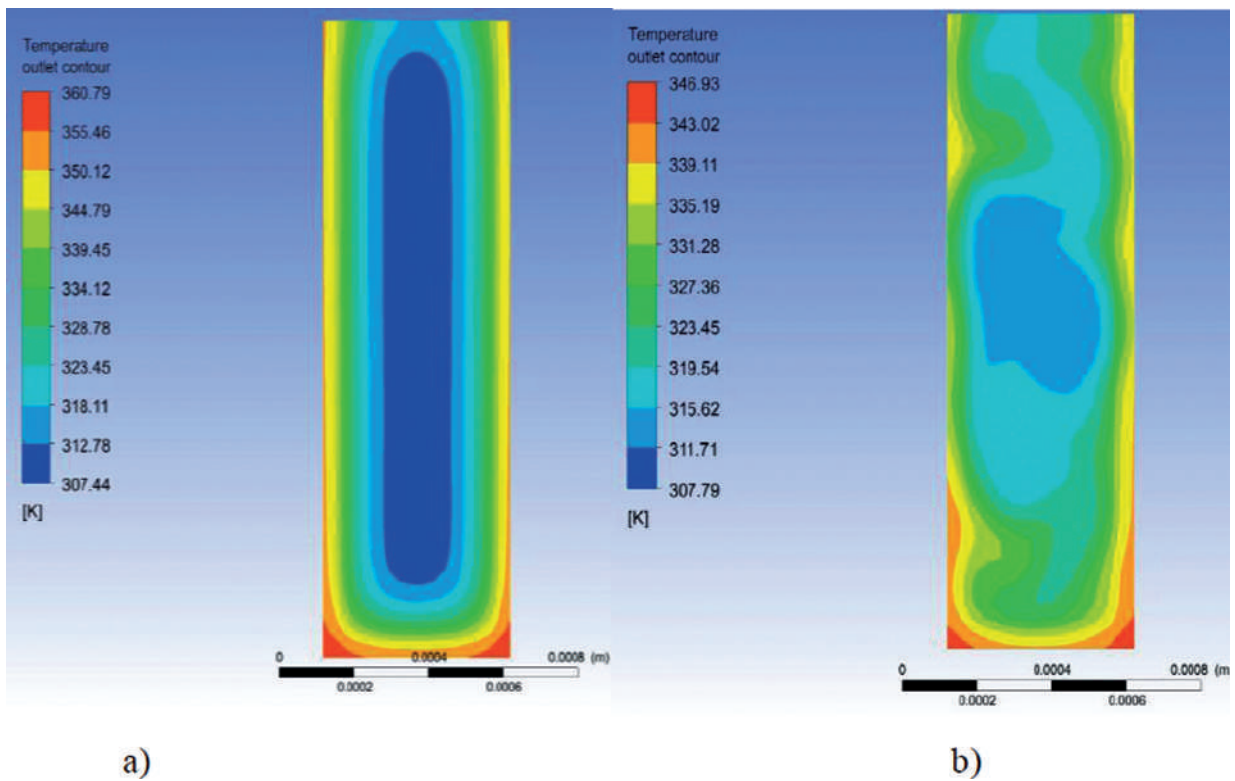


Figure 18: Temperature contour plot in the fluid region at outlet of a) Conventional MCHS b) PE-MCHS for heat flux of $100\text{W}/\text{cm}^2$.

pattern is repeated in the pin pitch region. The temperature distribution also has same variation in the entrance region for conventional and PE-MCHS along the channel wall. Further, the temperature keeps on increasing along the length of wall in conventional MCHS and reaches a maximum value of 347 K. In PE-MCHS, the temperature drops in the pin region and increase in between the pins forming

a pattern. The maximum temperature in PE-MCHS is 332 K and it reduces sharply in the pin region. The temperature gradient in the conventional MCHS is $1.55\text{ K}/\text{mm}$ while the same for PE-MCHS is $0.97\text{ K}/\text{mm}$.

The enhancement factor (eq. 10) evaluates the thermo-hydraulic performance of the enhanced MCHS in comparison with conventional MCHS. Figure 21 shows the

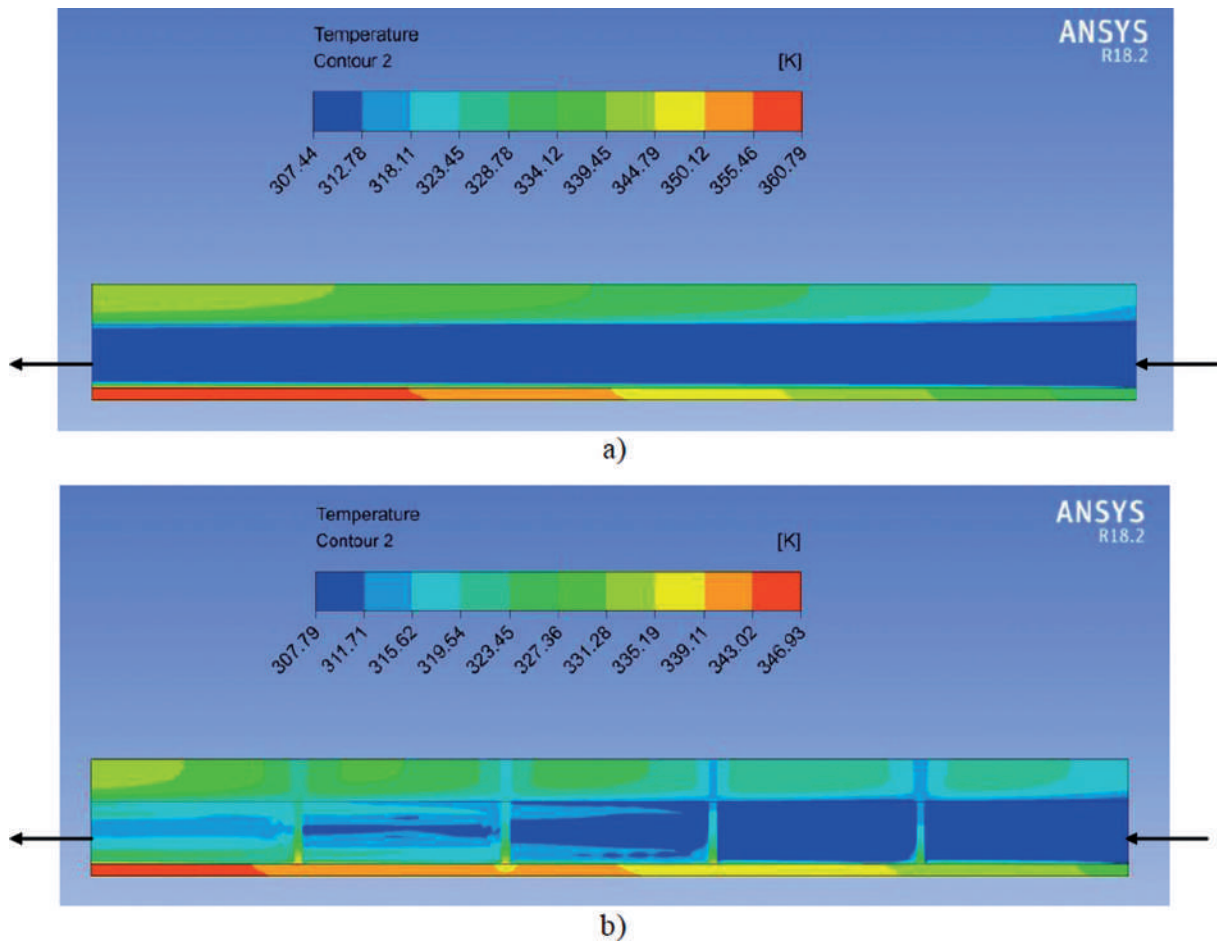


Figure 19: Temperature distribution in a vertical plane along channel length (YZ plane) for a) Conventional and b) PE-MCHS for Reynolds number of 745.

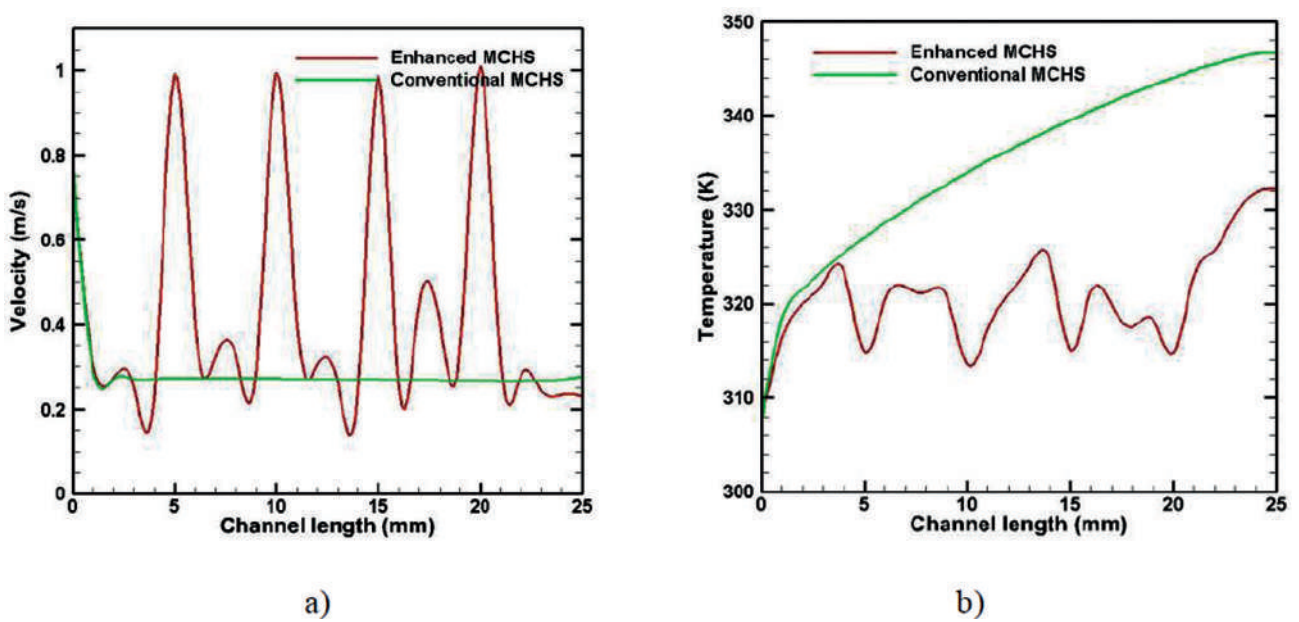


Figure 20: a) Velocity and b) Temperature distribution along the channel wall for conventional and PE-MCHS.

enhancement factor for heat flux of 100 and 200 W/cm². “Enhancement factor of more than one indicates an improvement in thermal performance over conventional MCHS”[1]. The enhancement factor initially increases with increase in Reynolds number and remains constant for higher Reynolds number. The reason for this can be due to the increase in Nusselt number with increase in Reynolds number, but with higher Reynolds number the pressure

drop negates the increase in Nusselt number. The average enhancement factor obtained is 1.24 for heat flux of 150 and 200 W/cm², for heat flux of 65 W/cm² the enhancement factor is 1.21 and for 100 W/cm² it is 1.23.

Correlations

Correlation for Nusselt number

Classical heat transfer relates the Nusselt number with Reynolds number and Prandtl number in previous pin-fin heat transfer correlations [34] and is given by

$$Nu = cRe^m Pr^n \tag{11}$$

where, c is the coefficient which accounts for the effect of geometrical parameters on heat transfer. The exponents’ m and n account for the effect of Reynolds number and Prandtl number on Nusselt number respectively. Effect of pin diameter on the thermo-hydraulic performance of MCHS is proposed in the form of correlation in this paper. The insertion of pins reduce the flow passage within the microchannel, which affects the heat transfer, hence the ratio of width of channel and pin diameter (Wc/Dp) is considered for the correlation. Proposed correlation showing effect of channel width to pin diameter ratio (Wc/Dp) on Nusselt number is given by

$$Nu = c \left(\frac{W_c}{D_p} \right)^j Re^m Pr^n \tag{12}$$

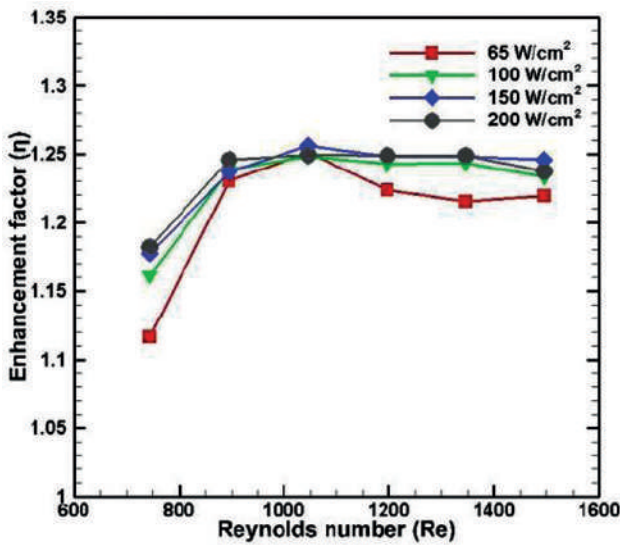
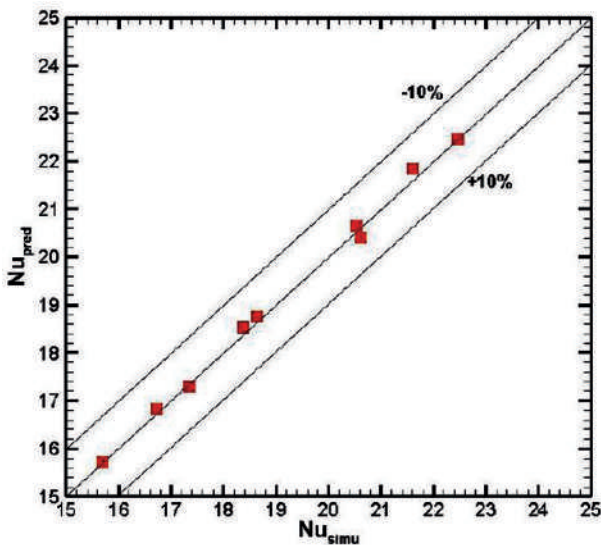
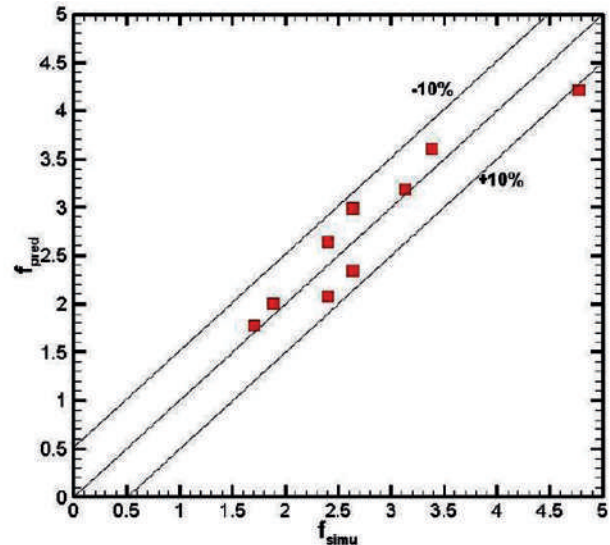


Figure 21: Enhancement factor at various Reynolds number for different heat flux.



a)



b)

Figure 22: Comparison of a) Nusselt number and b) Friction factor obtained by correlation with corresponding values obtained by simulation.

Multiple non-linear regression analysis is done to obtain the coefficients of Equation 12 as given below:

$$Nu = \left(\frac{W_c}{D_p} \right)^{-0.377} Re^{0.525} Pr^{-0.13} \quad (13)$$

Average mean error for Equation 13 is given by Equation 14 and has a value of 0.555%. Also the correlation coefficient is 0.998 and the R2 value is 0.999

$$MAE_{Nu} = \frac{1}{n} \sum_{k=1}^n \frac{abs(Nu_{sim} - Nu_{pred})}{Nu_{sim}} \times 100\% \quad (14)$$

Correlation for friction factor

Proposed correlation between ratio of channel width to pin diameter (W_c/D_p) and Reynolds number on friction factor is given by

$$f = C \left(\frac{W_c}{D_p} \right)^j Re^m \quad (15)$$

The coefficients of eq. 15 can be obtained by multiple nonlinear regression. The correlation obtained is given by

$$f = 555.5 \left(\frac{W_c}{D_p} \right)^{-0.847} Re^{-0.673} \quad (16)$$

Average mean error for Equation 16 is given by eq. 17 and has a value of 8.545%, and the correlation coefficient is 0.944 and the R2 value is 0.888

$$MAE_f = \frac{1}{n} \sum_{k=1}^n \frac{abs(f_{sim} - f_{pred})}{f_{sim}} \times 100\% \quad (17)$$

The range for W_c/D_p considered for the correlation is 1.667 to 4.0 while the range for Reynolds number considered is 745 to 895. Figure 22(a)&(b) shows the probability-probability plot which compares the simulated results with the ones predicted by correlations. Average mean error of less than 10 percent demonstrates good predictive capability of the newly developed correlations.

CONCLUSIONS

Numerical and experimental analysis of conventional and pin enhanced MCHS and its performance comparison is done in this paper and the findings are as follows:

1. The thermo-hydraulic performance of the new design of microchannel with pins inserted from top cover is similar to microchannel with conventional microchannel with pin-fins.

2. The performance of pins having diameter of 0.125 to 0.3mm (relative pin diameter $\gamma = 0.25$ to 0.6) are compared. Pins of 0.2mm diameter (relative pin diameter $\gamma = 0.4$) showed the best performance and are considered for further analysis.
3. The experimental results are in good agreement with the numerical results.
4. The velocity distribution is same in the entrance region for both MCHS but changes drastically due to the presence of pins. The thermal performance in PE-MCHS is higher than conventional MCHS. The temperature gradient observed along the channel wall is more in conventional MCHS than PE-MCHS.
5. The accompanying pressure drop due to the presence of pins in PE-MCHS is nearly two times that for the conventional MCHS. For PE-MCHS, the average enhancement factor obtained is 1.21 for heat flux of 65 W/cm², 1.23 for 100 W/cm², 1.24 for heat flux of 150 and 200 W/cm².
6. Correlations describing the relation between ratio of pin diameter to width of channel on Nusselt number and friction factor are proposed. The average mean error for Nusselt number and friction correlation is 0.555 % and 8.545 % respectively.

NOMENCLATURE

A	Area
C_p	Specific heat, (kJ/kg K)
D_h	Hydraulic diameter, (mm)
D_p	Diameter of pin (mm)
Hc	Height of channel (mm)
H	Heat transfer coefficient, (W/sq. m K)
K	Thermal conductivity (W/m K)
Lc	Total channel length, (mm)
\dot{m}	Mass flow rate, (kg/s)
Nu	Nusselt number
P	Pressure, (Pa)
q_w	Heat flux (W/cm ²)
Re	Reynolds number
T	Temperature, (K)
U	Velocity, (m/s)
W	Width (mm)

Greek

Δp	Pressure drop
H	enhancement factor
ΔT	Temperature difference
P	density, (kg/cubic m)
M	viscosity, (Pa s)

Subscripts

0	conventional
App	apparent
Ave	average
bottom	base

C	channel
Con	Contact surface
F	fluid
H	hydraulic
In	inlet
M	mean
Max	maximum
pred	predicted
S	surface
Sim	simulation
W	wall

Acronyms

MCHS	Microchannel heat sink
PE-MCHS	Pin enhanced microchannel heat sink
MAE	Average Mean error

DECLARATIONS OF INTEREST

None

ACKNOWLEDGEMENT

The authors would like to thank the Government College of Engineering Karad, India and AICTE Delhi, India for the facilities used for this work.

AUTHORSHIP CONTRIBUTIONS

Authors equally contributed to this work.

DATA AVAILABILITY STATEMENT

The authors confirm that the data that supports the findings of this study are available within the article. Raw data that support the finding of this study are available from the corresponding author, upon reasonable request.

CONFLICT OF INTEREST

The author declared no potential conflicts of interest with respect to the research, authorship, and/or publication of this article.

ETHICS

There are no ethical issues with the publication of this manuscript.

REFERENCES

- [1] Gaikwad V, Mohite S. Performance analysis of microchannel heat sink with secondary flows and flow disrupting pins. 2020;437–442.
- [2] Tuckerman DB, Pease RFW. High-performance heat sinking for VLSI. IEEE Electron Device Lett 1981;2:126–129. [CrossRef]
- [3] Knight RW, Hall DJ, Goodling JS, Jaeger RC. Heat sink optimization with application to microchannels. IEEE Trans Components Hybrids Manuf Technol 1992;15:832–842. [CrossRef]
- [4] Steinke M, Kandlikar S. Review of single-phase heat transfer enhancement techniques for application in microchannels, minichannels and microdevices. Int J Heat Technol 2004;22:3–11. [CrossRef]
- [5] Kosar A, Peles Y. Thermal-hydraulic performance of MEMS-based pin fin heat sink. J Heat Transf 2006;128:121. [CrossRef]
- [6] Colgan EG, Furman B, Gaynes M, Graham WS, LaBianca NC, Magerlein JH, et al. Practical implementation of silicon microchannel coolers for high power chips. IEEE Trans Components Packag Technol 2007;30:218–225. [CrossRef]
- [7] Hong F, Cheng P. Three dimensional numerical analyses and optimization of offset strip-fin microchannel heat sinks. Int Commun Heat Mass Transf 2009;36:651–656. [CrossRef]
- [8] Shafeie H, Abouali O, Jafarpur K, Ahmadi G. Numerical study of heat transfer performance of single-phase heat sinks with micro pin-fin structures. Appl Therm Eng 2013;58:68–76. [CrossRef]
- [9] Xie J, Yan H, Sundén B, Xie G. The influences of side-wall proximity on flow and thermal performance of a microchannel with large-row pin-fins. Int J Therm Sci 2019;140:8–19. [CrossRef]
- [10] Rubio-Jimenez CA, Kandlikar SG, Hernandez-Guerrero A. Numerical analysis of novel micro pin fin heat sink with variable fin density. IEEE Trans Components Packag Manuf Technol 2012;2:825–833. [CrossRef]
- [11] Yadav V, Baghel K, Kumar R, Kadam ST. Numerical investigation of heat transfer in extended surface microchannels. Int J Heat Mass Transf 2016;93:612–622. [CrossRef]
- [12] Jia Y, Xia G, Li Y, Ma D, Cai B. Heat transfer and fluid flow characteristics of combined microchannel with cone-shaped micro pin fins. Int Commun Heat Mass Transf 2018;92:78–89. [CrossRef]
- [13] Ansari D, Kim KY. Hotspot thermal management using a microchannel-pinfin hybrid heat sink. Int J Therm Sci 2018;134:27–39. [CrossRef]
- [14] Chai L, Xia G, Wang L, Zhou M, Cui Z. Heat transfer enhancement in microchannel heat sinks with periodic expansion-constriction cross-sections. Int J Heat Mass Transf 2013;62:741–751. [CrossRef]
- [15] Kumar P. Numerical investigation of fluid flow and heat transfer in trapezoidal microchannel with groove structure. Int J Therm Sci. 2019;136:33–43. [CrossRef]
- [16] Duryodhan VS, Singh A, Singh SG, Agrawal A. Convective heat transfer in diverging and converging

- microchannels. *Int J Heat Mass Transf* 2015;80:424–438. [CrossRef]
- [17] Yong JQ, Teo CJ. Mixing and heat transfer enhancement in microchannels containing converging-diverging passages. *J Heat Transfer* 2014;136:41704. [CrossRef]
- [18] Lan J, Xie Y, Zhang D. Flow and heat transfer in microchannels with dimples and protrusions. *J Heat Transfer* 2012;134:21901. [CrossRef]
- [19] Xu M, Lu H, Gong L, Chai JC, Duan X. Parametric numerical study of the flow and heat transfer in microchannel with dimples. *Int Commun Heat Mass Transf* 2016;76:348–357. [CrossRef]
- [20] Lu G, Zhai X. Analysis on heat transfer and pressure drop of a microchannel heat sink with dimples and vortex generators. *Int J Therm Sci* 2019;145:105986. [CrossRef]
- [21] Xie G, Zhang F, Sundén B, Zhang W. Constructal design and thermal analysis of microchannel heat sinks with multistage bifurcations in single-phase liquid flow. *Appl Therm Eng* 2014;62:791–802. [CrossRef]
- [22] Shen H, Wang C-C, Xie G. A parametric study on thermal performance of microchannel heat sinks with internally vertical bifurcations in laminar liquid flow. *Int J Heat Mass Transf* 2018;117:487–497. [CrossRef]
- [23] Zunaid Mohammad SA, Jindal A, Gakhar D. Numerical study of pressure drop and heat transfer in a straight rectangular and semi cylindrical projections microchannel heat sink. *J Therm Eng* 2017;3:1453–1465. [CrossRef]
- [24] Belhadj RS, Bouchenafa R, Saim R. A numerical study of forced convective flow in microchannels heat sinks with periodic expansion-constriction cross section. *J Therm Eng* 2018;4:1912–1925. [CrossRef]
- [25] Li YF, Xia GD, Ma DD, Jia YT, Wang J. Characteristics of laminar flow and heat transfer in microchannel heat sink with triangular cavities and rectangular ribs. *Int J Heat Mass Transf* 2016;98:17–28. [CrossRef]
- [26] Chai L, Wang L, Bai X. Thermohydraulic performance of microchannel heat sinks with triangular ribs on sidewalls – Part 1: Average fluid flow and heat transfer characteristics. *Int J Heat Mass Transf* 2019;128:634–648. [CrossRef]
- [27] Lee YJ, Lee PS, Chou SK. Numerical study of fluid flow and heat transfer in the enhanced microchannel with oblique fins. *J Heat Transfer* 2013;135:41901. [CrossRef]
- [28] Kuppasamy NR, Saidur R, Ghazali NNN, Mohammed HA. Numerical study of thermal enhancement in micro channel heat sink with secondary flow. *Int J Heat Mass Transf* 2014;178:216–223. [CrossRef]
- [29] Gaikwad V, Mohite S, Shinde S, Dherange M. Enhancement in thermo-hydraulic performance of microchannel heat sink with secondary flows of leaf venation pattern. *J Therm Eng* 2020;469:12032. [CrossRef]
- [30] Meral ZK, Parlak N. Experimental research and cfd simulation of cross flow microchannel heat exchanger. *J Therm Eng* 2021;7:270–283. [CrossRef]
- [31] Madani K, Ben Maad R, Abidi-Saad A. Numerical investigation of cooling a ribbed microchannel using nanofluid. *J Therm Eng* 2018;4:2408–2422. [CrossRef]
- [32] Chai L, Xia GD, Wang HS. Numerical study of laminar flow and heat transfer in microchannel heat sink with offset ribs on sidewalls. *Appl Therm Eng* 2016;92:32–41. [CrossRef]
- [33] Xia GD, Jia YT, Li YF, Ma DD, Cai B. Numerical simulation and multiobjective optimization of a microchannel heat sink with arc-shaped grooves and ribs. *Numer Heat Transf Part A Appl* 2016;70:1041–1055. [CrossRef]
- [34] Mei D, Lou X, Qian M, Yao Z, Liang L, Chen Z. Effect of tip clearance on the heat transfer and pressure drop performance in the micro-reactor with micro-pin-fin arrays at low Reynolds number. *Int J Heat Mass Transf* 2014;70:709–718. [CrossRef]
- [35] Qu W, Mudawar I. Experimental and numerical study of pressure drop and heat transfer in a single-phase micro-channel heat sink. *Int J Heat Mass Transf* 2002;45:2549–2565. [CrossRef]